Chapter 1

Colloidal Lithography

Ye Yu and Gang Zhang

Additional information is available at the end of the chapter

http://dx.doi.org/10.5772/56576

1. Introduction

The advent of nanoscience and nanotechnology has led to tremendous enthusiasm of researchers from different scientific disciplines such as physics, chemistry, and biology to engage with nanostructures with the intent of pursuing the innovative property derived from the nanometer dimension. In this context, fabrication of nanostructures accordingly becomes an increasing demand nowadays. Obviously, low-throughput and expensive maskless lithography is a less accessible choice for chemists, physicists, material scientists, and biologists. The success of extending mask-assisted lithography beyond microelectronics workshops is largely limited by the mask design and preparation. Recently a host of effort has been devoted to develop non-conventional lithographic techniques especially integrated with a bottom-up nanochemical procedure for surface patterning with low cost, flexible processing capability, and high throughput. However, most of the non-conventional lithographic techniques require an assistance of conventional lithographic techniques such as photolithography to design and make masks or masters. To develop ingenious, cheap, and non-lithographic ways to make masks or masters with high resolution (below 100 nm), a great deal of self-assembly nanostructures have been recruited for masking, including laterally structured Langmuir–Blodgett monolayers, liquid crystalline structures of surfactants, micro-phase separation structures of block copolymers, and self-assembly of proteins and nanoparticles.

Monodisperse colloidal particles with size ranging from tens of nanometers to tens of micrometers can be easily synthesized via wet chemistry ways such as emulsion polymerization and sol-gel synthesis. Due to the size and shape monodispersity, they can self-assemble into a two dimensional (2D) and three dimensional (3D) extended periodic array, usually referred to as colloidal crystal. Colloidal crystals are usually characterized by a brilliant iridescence arising from the Bragg reflection of light by their periodic structures. Despite the beauty, the iridescent color has recently inspired the explosive study of fabrication of 3D colloidal crystals or inverse opals – 3D inverted replication of the crystals – for pursuing a complete energy bandgap to

manipulate electromagnetic waves, similar to that to do to electrons in semiconductors. Before being used as photonic materials, both the ordered arrays of solid particles and those of the interstices between the particles of colloidal crystals have already been used as masks or templates for surface patterning via for instance etching or deposition of materials. This bottom-up masking methodology has recently gained increasing attention for surface patterning due to the processing simplicity, the low cost, the flexibility of extending on various substrates with different surface chemistry and even curvatures, the ease of scaling down the feature size below 100 nm. In the present chapter, we refer to as various surface patterning processes based on use of colloidal crystals as masks as a whole as colloidal lithography (CL), overview the processing principles, and survey the recent advances.

2. Colloidal masks

The success of using colloidal crystals as masks for surface patterning is determined by the capability of directing self-assembly of colloidal particles and manipulating the crystal packing structures. Provided their size and shape are monodisperse, colloidal particles can be readily to self-assemble into long-range ordered arrays with a hexagonal packing, driven simply by entropic depletion and gravity. Up to date a variety of colloidal crystallization techniques – with and without the aid of templates – have successfully been developed to implement colloidal crystallization in a controlled fashion [1-3]. Due to enormous numbers of publications on colloidal crystallization and immense diversity of crystallization techniques reported thus far and especially by taking into account that colloidal lithography relies on masking of single layers or double layers of colloidal crystals, this section is centered mainly on techniques for 2D colloidal crystallization developed thus far.

2.1. Simple colloidal masks

2.1.1. Sedimentation

Sedimentation is a natural way for colloidal crystallization. In dispersion colloidal particles tend to settle out of the fluid under gravity and to accumulate and precipitate on a wall, which can be described by Stokes' law. This sedimentation process can be used to grow colloidal crystals with high quality, and the crystal thickness can be tuned by the particle concentration. However, the sedimentation time is always up to several hundreds of hours; time-consuming is a big drawback of this technique [4-6].

At the beginning of 1990's Nagayama's group has commenced a systematic study of sedimentation of colloidal particles in the presence of strongly attractive capillary forces [7]. With the help of optical microscopy and using a Teflon ring to confine the dispersions of colloidal particles, they have directly observed the particle sedimentation dynamics on a solid substrate. Their observations suggest a two-stage mechanism for 2D colloidal crystallization: 1) nucleation and 2) crystal growth (Fig. 1) [7]. Micheletto's group has fabricated 2D colloidal crystals

http://dx.doi.org/10.5772/56576

on a solid substrate via sedimentation by tilting the substrate about 9° and keeping the system temperature constantly using a Peltier cell [8].

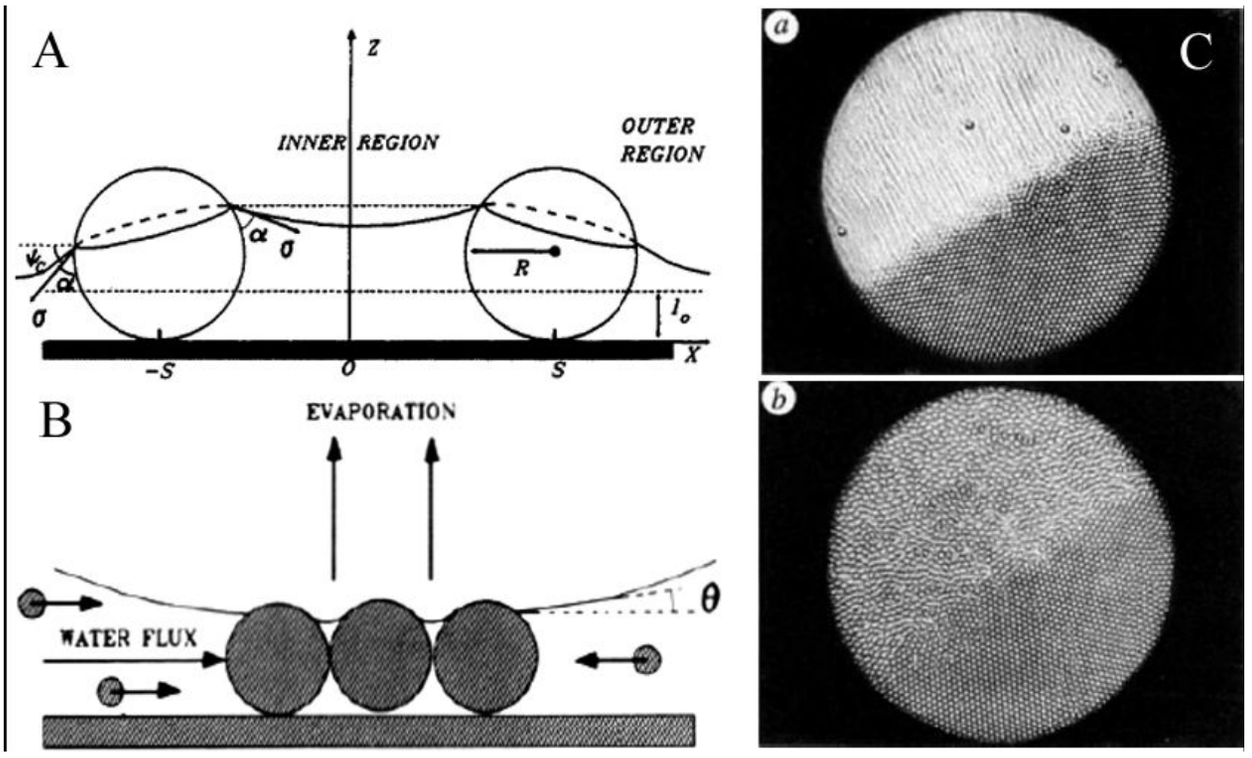

Figure 1. A) Two spheres partially immersed in a liquid layer on a horizontal solid substrate. The deformation of the liquid meniscus gives rise to interparticle attraction. (B) Convective flux toward the ordered phase due to the water evaporation from the menisci between the particles in the 2D array. (C) Photographs of 2D-crystal growth. Reprinted with permission [7].

2.1.2. Vertical deposition

When a supporting substrate is held vertically in a suspension of colloidal particles, moving the front of the suspension flow either by the solvent evaporation or by withdrawing the substrate out of the suspension can pin colloidal particles on the substrates – nucleation – and the convective transfer of the particles from the bulk phase to the drying front – crystallization (Fig. 2) [9]. The thickness of colloidal crystals obtained via vertical deposition is dependent on the ratio of the thickness of the liquid films remaining of supporting substrates to the diameter of the colloidal particles [9]. When the ratio is far larger than 1, 3D colloidal crystals are obtained with high quality; the crystal thickness can be tuned by the particle concentration [10]. When the ratio is comparable to or smaller than 1, 2D colloidal crystals can be obtained [9]. Vertical deposition may allow formation of large-area crack-free colloidal crystals provided the suspensions of colloidal particles wet well supporting substrates, there is no interaction between the particles and the substrates, the suspensions are sufficiently stable and the solvent evaporation is well controlled [9].

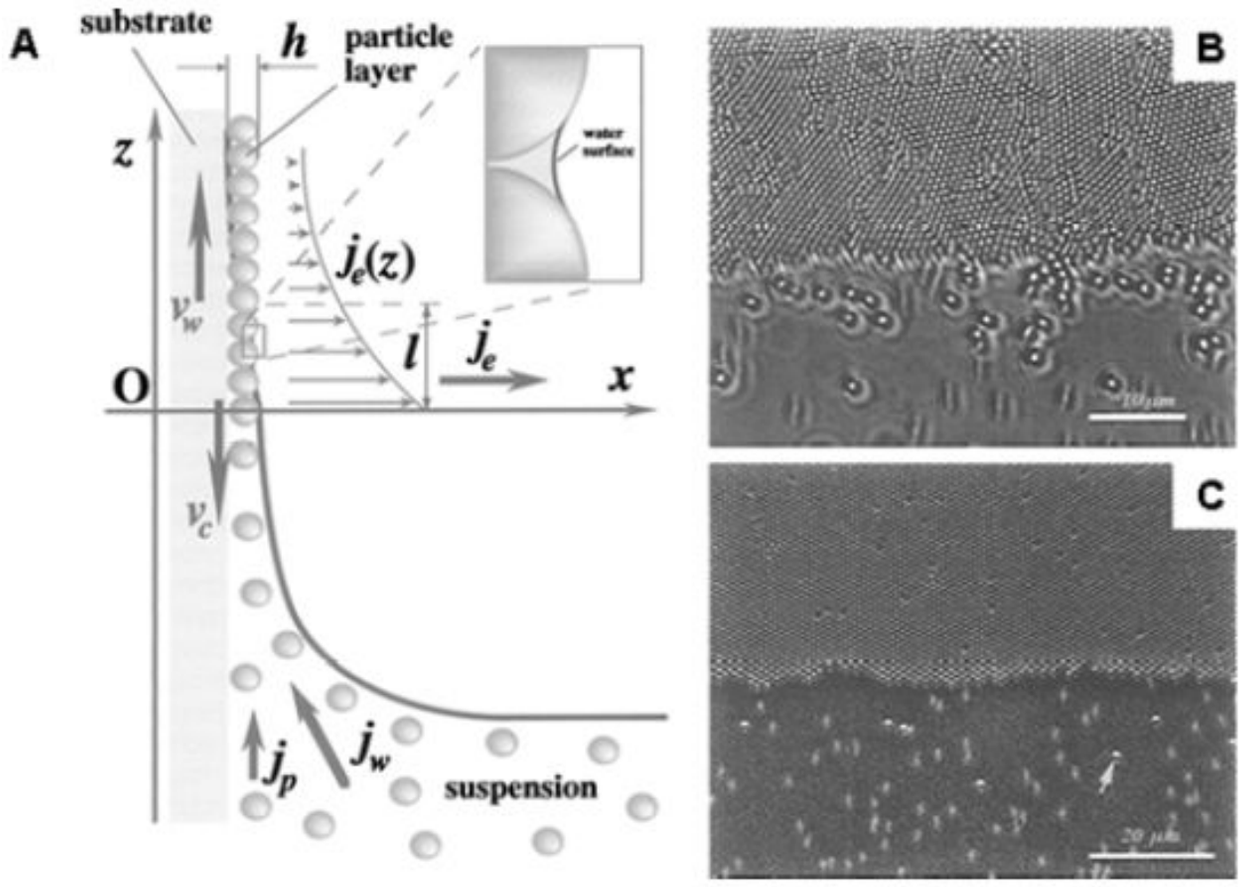

Figure 2. A) Sketch of the particle and water fluxes in the vicinity of monolayer particle arrays growing on a substrate plate that is being withdrawn from a suspension. The inset shows the menisci shape between neighbouring particles. (B and C) A part of the leading edge of a growing monolayer particle array. The upper-half of the photographs shows the formations of (B) differently oriented small domains of ordered 814-nm particles and (C) a single domain of ordered 953-nm particles. The lower-half shows particles dragged by the water flow toward the forming monolayer. Reprinted with permission [9].

Dip-coating is a fast and dip-coater assisted variant of vertical deposition [11]. Besides, a number of techniques have been developed to improve the efficiency and quality of colloidal crystallization via vertical deposition, such as variable-flow deposition [12], isothermal heating evaporation-induced self-assembly [13], two-substrate deposition [14], reduction of the humidity fluctuation [15], adjustment of the meniscus shape [16], temperature-induced convective flow [17] and vertical deposition with a tilted angle [18]. The maximal size of colloidal particles used for vertical deposition is limited by the particles sedimentation of colloidal particles, for instance 400-500 nm for silica particles and 1 μm for polystyrene particles. To compete with sedimentation, Kitaev and Ozin have used low pressure to accelerate the solvent evaporation, and successful growth of large-area 2D binary colloidal crystals with the diameter ratios of the large particles to the small ones in the range of 0.175 to 0.225 (Fig. 3) [19].

Vertical deposition has recently been extended to stepwise growth of 2D colloidal crystals with large and small colloidal particles on a substrate [20, 21]. In their procedure, the 2D colloidal

http://dx.doi.org/10.5772/56576

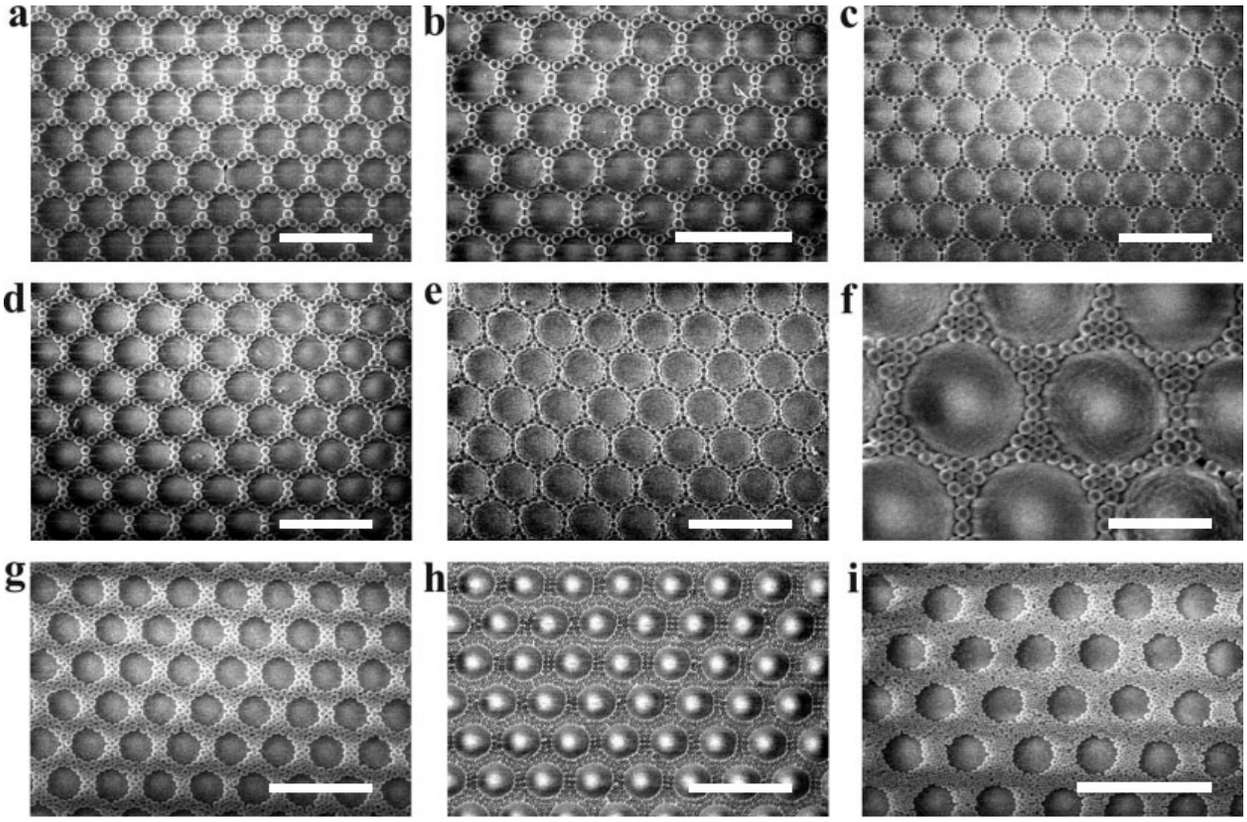

Figure 3. Library of surface micropatterns produced by accelerated evaporation co-assembly of binary dispersions of monodisperse microspheres with large size ratio and imaged with field emission scanning electron microscopy. Larger spheres of all binary dispersions were PS latex of size, d_L= 1.28 μm, while varying their volume fraction (φ_L), the volume fraction (φ_S), and size (d_S) of smaller spheres. Scale bars in (a-e) and (g-i) are 3 μm and that in (f) is 1 μm. Reprinted with permission [19].

crystal of the larger particles firstly formed on the substrate is used to template the growth of the 2D colloidal crystal of the smaller particles. By deliberately tuning the concentration of the small particle suspension, binary colloidal crystals with the stoichiometric ratios of large to small particle sizes of 1:2, 1:3, 1:4, or 1:5 have been constructed [20, 21].

2.1.3. Spin coating

Spin coating was the first technique for growth of 2D colloidal crystal masks for colloidal lithography due to the fact that it allows easy and quick formation of 2D crystals over large area [22]. The long range ordering degree of 2D colloidal crystals obtained via spin coating can be improved by increasing the wettability of the suspensions of colloidal particles on supporting substrates by for instance adding ethylene glycol into the suspension [23]. However, the spin coating is a process far more complicated than it appears and the underlying mechanism remains in debate. Rehg and Higgins have conducted a theoretical analysis of the physics governing spin coating of a colloidal particle suspension on a planar substrate [24]. Jiang and Mcfarland have succeeded in fabrication of wafer scale long-rang ordered and non-close-packed 2D and 3D colloidal crystals by spin coating of highly viscous triacrylate

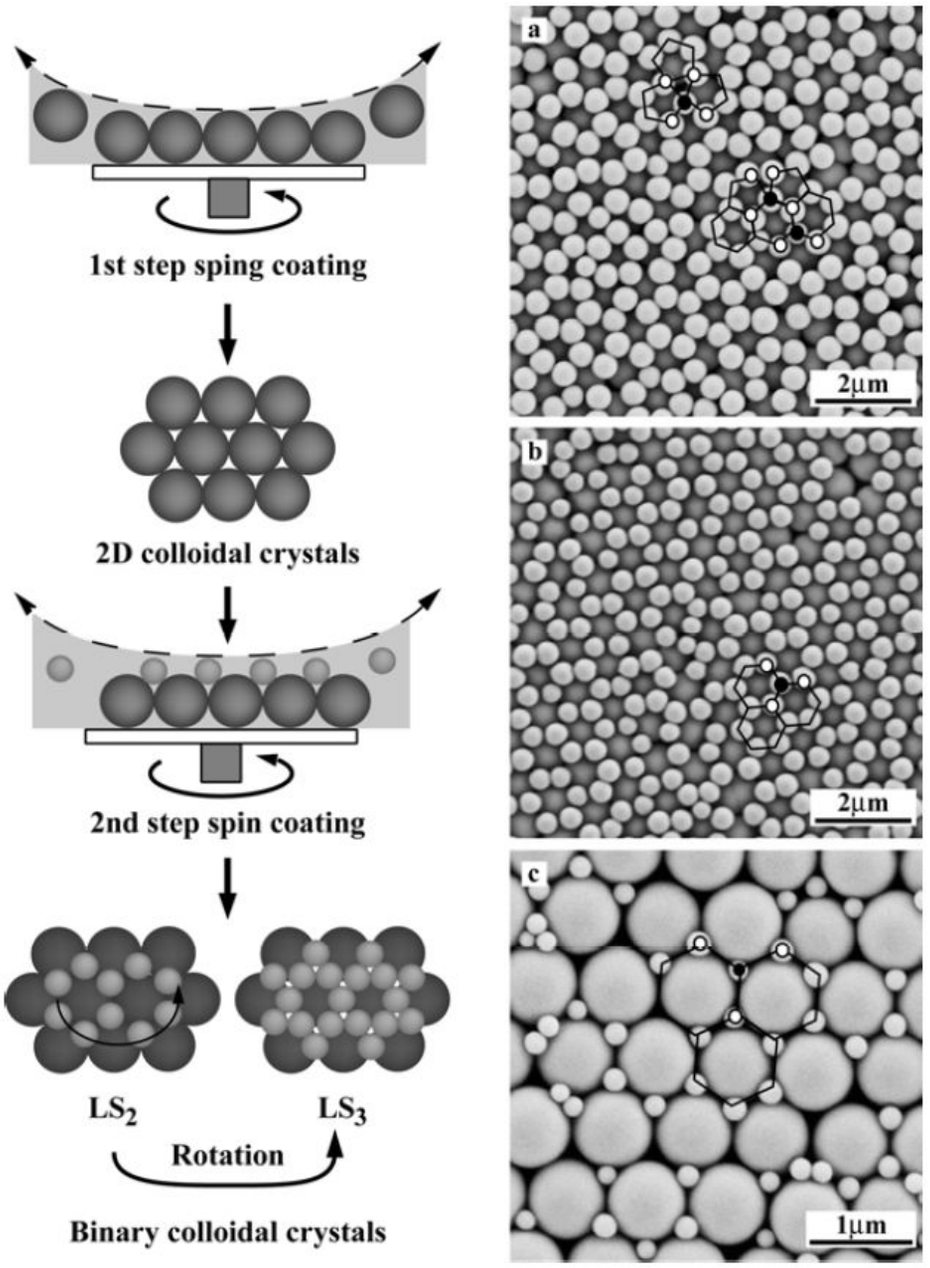

Figure 4. Left panel: Illustration of the procedure used to fabricate binary colloidal crystals by stepwise spin coating. Right panel: SEM micrographs of the binary colloidal crystals produced by stepwise spin coating at a spin speed of 3000 rpm, in which 519 nm (a), 442 nm (b), and 222 nm silica spheres (c) were confined within the interstices between hexagonal close packed 891 nm silica spheres. Reprinted with permission [27].

suspension of silica particles and subsequent polymerization of triacrylate, followed by partial removal of the polymer matrices [25, 26]. Wang and Möhwald have developed a stepwise spin coating protocol to consecutively deposit large and small colloidal particles into binary colloidal crystals, in which the interstitial arrays in the 2D colloidal crystal of the large particles are used to template the deposition of the small particles due to the spatial and depletion entrapment (Fig. 4) [27].

2.1.4. Colloidal crystallization at interface

Using the water/air interface as a platform for molecular self-assembly has been extensively studied. Langmuir-Blodgett (LB) technique has been proved as a powerful and versatile way to organize amphiphilic molecules (referring molecules that are hydrophobic on one end and hydrophilic on the other end) to macroscopic monolayer films at the water/air interface and transfer the films to solid substrates in a controlled manner [28]. It is also well studied but less recognized that in a biphasic system, e.g. water/oil, colloidal particles behave rather similar to amphiphilic molecules; they thermo- dynamically prefer to attach to the interface [29]. Due to this analogy, the water/air interface has been extended to support self-assembly of colloidal particles. Pieranski has conducted the first deliberate microscopic observation of 2D colloidal crystallization at the water/air interface and hypothesized the repulsive interaction between the dipoles of colloidal particles trapped at the interface due to the asymmetric charge distribution on the particle surface drives the particles to self-assemble into an ordered array (Fig. 5) [30]. Park *et al.* have developed heat-assisted interfacial colloidal crystallization, while the success of their technique relies on the convective flow generated during heating rather than the interface activity of colloidal particles [31]. Once 2D colloidal crystals are formed at the water/air interface, the LB technique has been used to transfer of them on different substrates [32-35]. Of significance is that the LB technique allows repetition of transfer of 2D colloidal crystals on a substrate into 3D colloidal crystals with precisely defined layer numbers [35].

Colloidal monolayers with high order and increased complexity beyond plain hexagonal packing geometries are useful for 2D templating of surface nanostructures and lithographic applications. Weiss and co-workers developed binary colloidal monolayers featuring a close-packed monolayer of large spheres with a superlattice of small particles in a single step using a Langmuir trough [36].

As compared with the water/air interface, the water/oil interface is a much better platform to trap colloidal particles due to the relatively low interfacial tension [29]. Thus, water/oil interfaces have been used for growth of 2D colloidal crystals [37, 38], while transfer of the resulting 2D colloidal crystals to solid substrates remains problematic. Besides water/air interfaces, air/water/air interfaces have also been utilized for colloidal crystallization. Velikov and coworkers have studied of colloidal crystallization in thinning foam films [39]. Using air/water/air interfaces for crystallization, Wang and co-workers have successfully obtained free-standing and crack-free colloidal crystal films with sizes over several square millimeters [40]. Instead of water/air interface, Zental and co-workers have used the interface between melted germanium and air for colloidal crystallization and obtained crack-free colloidal crystals [41].

2.2. Complex colloidal masks

2.2.1. Deformed colloidal masks

In general, polymers undergo a second-order phase transition from hard glassy state to soft rubbery state above a glass transition temperature (Tg) due to the free-volume change between the polymer chains. Therefore, annealing slightly above Tg can cause deformation of spherical

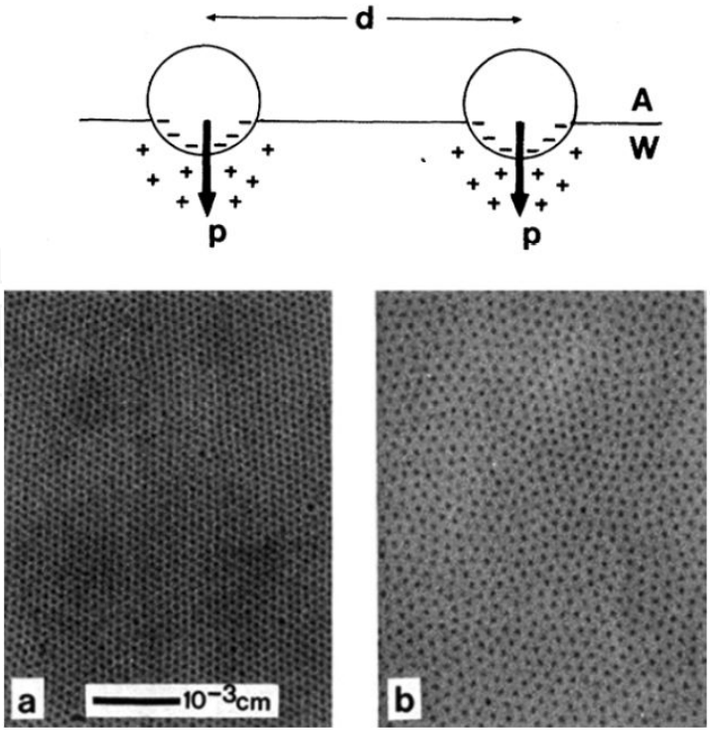

Figure 5. Upper panel: Schematic of the model of interaction of colloidal particles at the water (W)/air (A) interface. Lower panel: Photographs of polystyrene spheres (black dots) trapped at water/air interface. (a) Crystalline structure; (b) disordered structure. Reprinted with permission [30].

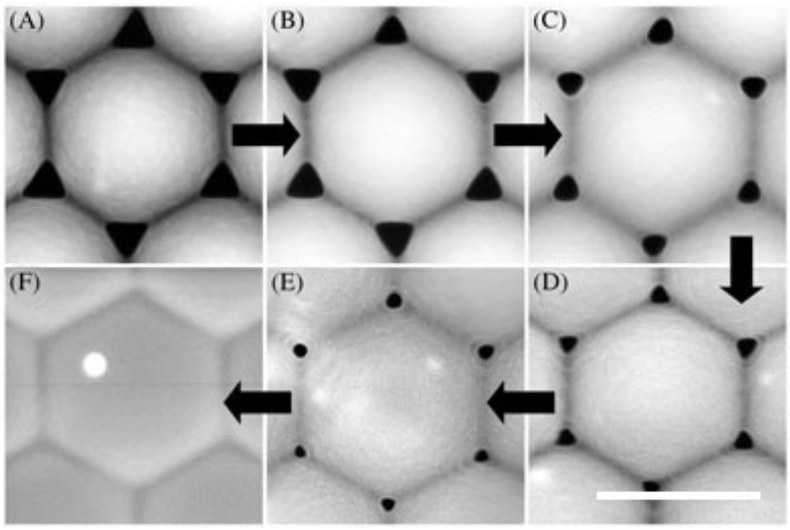

Figure 6. Precise control of the degree of annealing is achieved via adjustment of the number of microwave exposures: A 540 nm PS latex mask annealed in 25 mL of water/EtOH/acetone mixture by A) 1, B) 2, C) 4, D) 6, E) 7, and F) 10 microwave pulses. Scale bar: 500 nm. Reprinted with permission [43].

polymeric beads. It is demonstrated that microwave radiation can much more precisely control the deformation of spherical polymer particles by adjusting the microwave intensity than heating in oven [42].

Giersig and coworkers have recently developed a new annealing approach – using microwave pulse to heat polystyrene (PS) microspheres in a mixture of good and poor solvents for PS, which allows not only reduction of the sizes of the interstices of 2D PS colloidal crystals but also deformation of their geometry from triangular to rodlike, while preserving the interparticle spacing and packing order of the original crystals (Fig. 6) [43]. Recently, Yang *et al.* have demonstrated a photolithographic process to produce hierarchical arrays of nanopores or nanobowls with using colloidal crystals of photoresist particles [44]. In the case of inorganic particles, deformation is hard to achieve by thermal annealing. Polman and coworkers have successfully deformed silica@Au core-shell microspheres to oblate ellipsoids by using high energy ion irradiation due to the fact that the ion-induced deformation of the silica core is counteracted by the mechanical constraint of the gold shell [45]. Vossen and coworkers have recently reported that silica particles undergo anisotropic deformation under ion bombardment due to expansion in the plane perpendicular to the ion beam [46].

2.2.2. Colloidal masks derived from modified colloidal particles

Many specific colloidal masks have been made using methods mentioned above, usually utilizing one or two kinds of spherical colloidal particles as building blocks. Colloidal particles with anisotropic interactions are expected to enable a wide range of materials with novel optical and mechanical properties. While the self-assembly of spherical particles into periodic structures is relatively robust and well-characterized, the phase space describing the self-assembly of anisotropic particles is vast and has been only partially explored. It includes phases that are impossible for spherical particles to form, including gyroids, simple cubic lattices, and plastic crystals.

Eric R. Dufresne and co-workers demonstrated the use of an external electric field to align and assemble the dumbbells to make a birefringent suspension with structural color. In this way, dumbbells combine the structural color of photonic crystals with the field addressability of liquid crystals. In addition, if the solvent is removed in the presence of an electric field, the particles self-assemble into a novel, dense crystalline packing hundreds of particles thick, which was shown in Fig. 7 [47].

3. Colloidal lithography

3.1. Controllable etching

When a 2D colloidal crystal is formed on a solid substrate, the interstices between the solid particles can used as masks for reactive ions to create patterned bumps or pores on the substrate. In the beginning of 1980's Deckmann and Dunsmuir have pioneered the work of etching of a colloidal crystal into a textured surface using a reactive ion beam (RIE) [48]. Since then, reactive ion etching (RIE) has been widely used to interdependently reduce the particle sizes and thus widen the interstitial space in 2D colloidal crystal masks and eventually turn close-packing structures of the crystals to non-close packing one (vide infra). RIE in 3D colloidal crystals is an anisotropic process as the upper layers act as shadow masks for etching

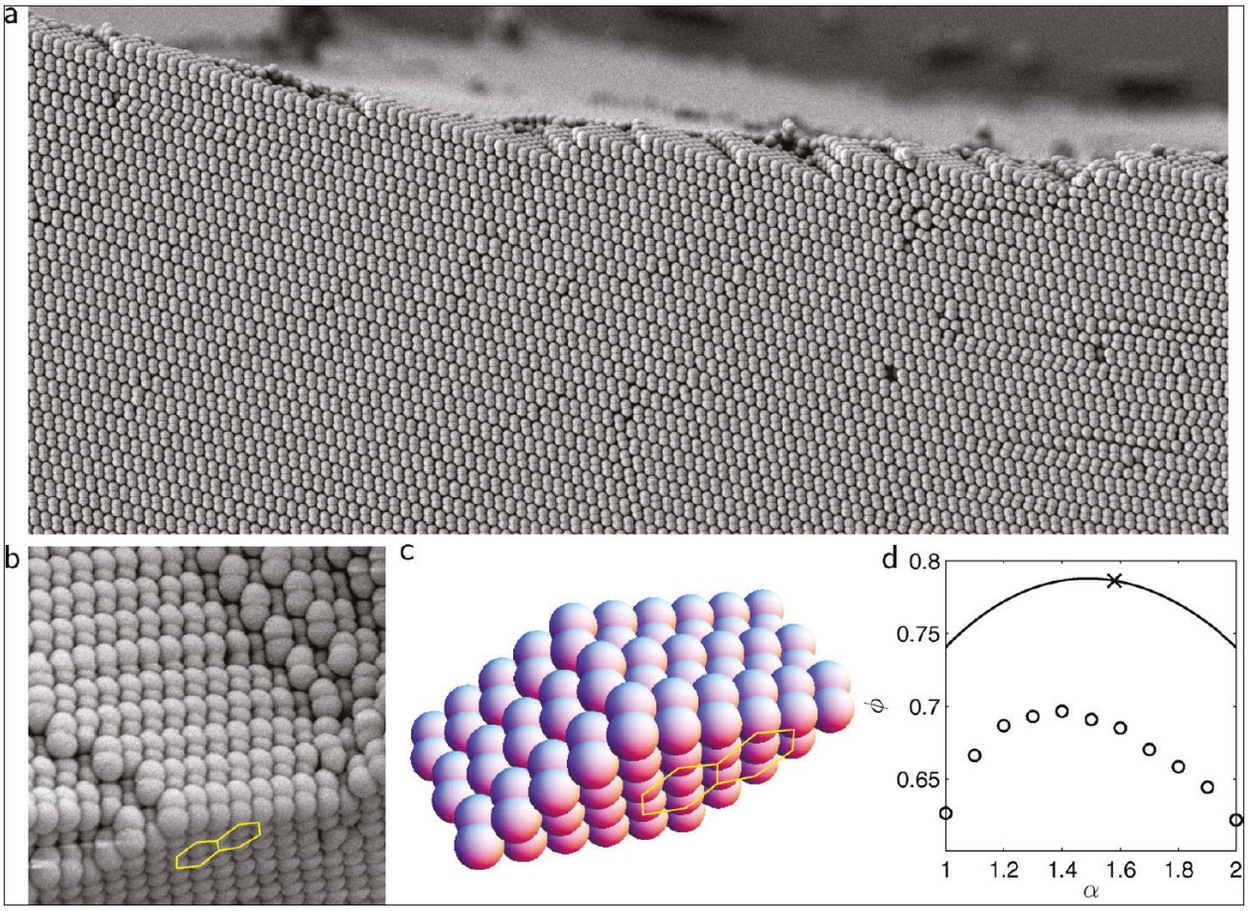

Figure 7. Crystal structure of suspension dried in an AC electric field. (a) SEM image of crystal formed by drying a suspension of dumbbells in the presence of an electric field. The field of view is 27 μm across. (b) SEM image highlighting crystal structure. Two adjoining hexagons formed by the dumbbell lobes are highlighted by the yellow hexagons. The field of view is 3.6 μm across. (c) Model of the crystal structure suggested by SEM images. Two adjoining hexagons are highlighted and correspond to the highlighted facet in (b). (d) Packing fraction versus aspect ratio for crystalline structures (line) and random, jammed packings (circles) generated from numerical simulations described in the Methods section. Reprinted with permission [47].

the lower layer particles. This anisotropic RIE can turn spherical particles to non-spherical particles, and the particle shapes and the hierarchical nanostructures obtained so strongly depends on the stacking sequence of the colloidal crystals, the crystal orientation relative to the substrate, the number of colloidal layers, and the RIE conditions (Fig. 8) [49]. Of most significance is that the anisotropic RIE paves a new way to machine the surfaces of colloidal particles. Such as nanopores arranged in threefold or fourfold symmetry, depending on the crystalline orientation of the original colloidal crystals, were machined on PS particles [50-52].

Forests of silicon pillars with diameters of sub-500 nm and an aspect ratio of up to 10 were have been fabricated by firstly conduct O_2 RIE to turn close-packed PS particle monolayers to non-close packed on and subsequently conduct a "Bosch" process to etch the supporting silicon wafers [53]. Sow *et al.* have demonstrated the characteristic features of a RIE silicon substrate using a PS colloidal crystal mask and produced a double dome structure by simultaneous etching of the mask and the regions beneath the particles [54]. As compared with convention-

http://dx.doi.org/10.5772/56576

ally used polymer masks such as photoresists removed by organic developers, colloidal masks can be removed easily by ultrasonication and thus cause less damage to nanostructured substrates obtained via RIE. Ordered arrays of polyacrylic acid domes have been fabricated by using 2D PS colloidal crystals as masks for O_2 RIE of the polymeric films; the removal of the PS masks has no damage to the surface chemistry and the structure of the resulting polymeric domes, thus enabling conjugation of proteins [55]. 2D PS colloidal crystals have been also used as masks for dry etching of SiO_2 slides to create periodic arrays of nanoplates, which can be transferred onto polymer films by imprinting [56]. Using colloidal crystals as masks for catalytic etching, Zhu *et al.* have fabricated large-scale periodic arrays of silicon nanowires and the diameters and heights of the nanowires and the center-to-center distances between the nanowires can be accurately controlled [57]. Using colloidal crystals as masks to create arrays of nanopores on supporting solid substrates via RIE, followed by consecutively deposition of gold films and removal of the colloidal masks, Ong *et al.* have fabricated 2D ordered arrays of gold nanoparticles nested in the nanopores of the templated substrate [58]. One potential extension of having gold nanoparticles confined in nanopores is to use them as catalysts for growth of nanowires of other materials such as ZnO nanowires.

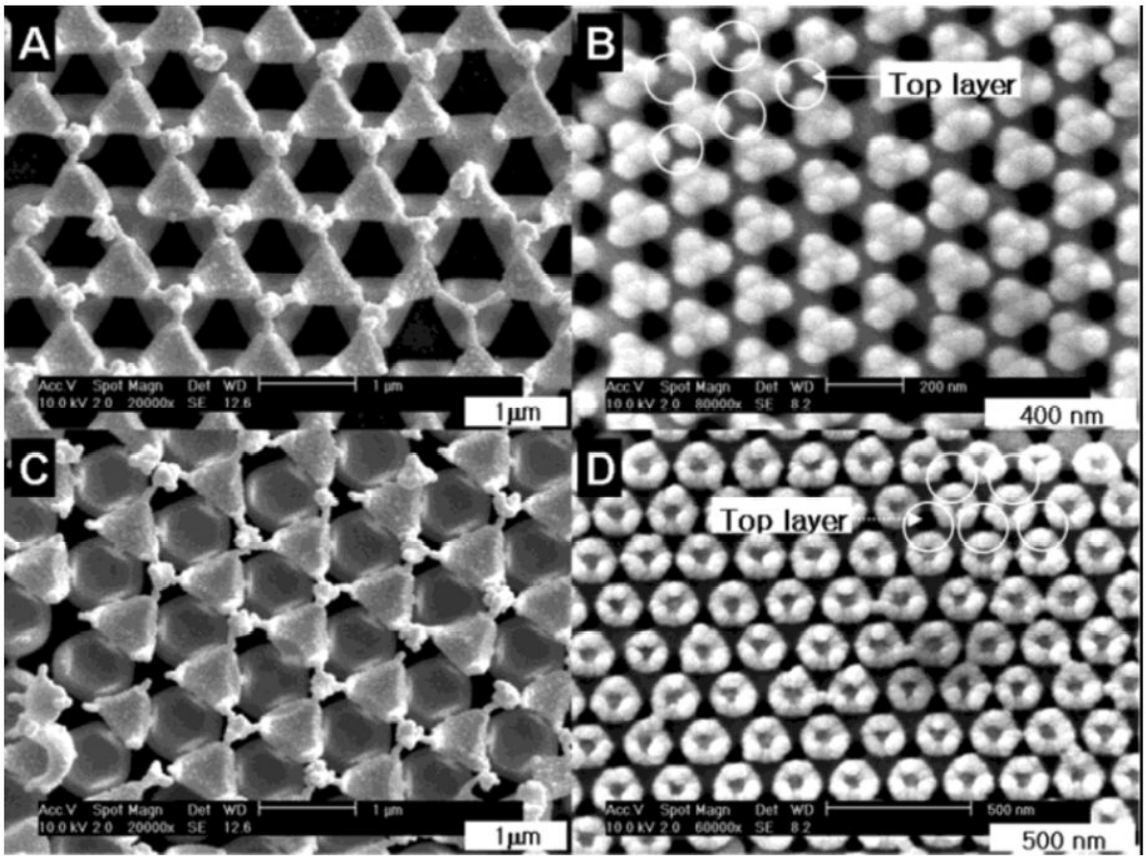

Figure 8. Modification of a mask using RIE for the fabrication of binary and ternary particle arrays with nonspherical building blocks. (a) and (b) Triangle arrays using binary and ternary colloidal spheres with an hcp arrangement. (c) and (d) Polygonal structures produced from colloidal layers with the (111) plane and the (100) plane of the *fcc* structure, respectively. Reprinted with permission [49].

3.2. Controllable deposition

3.2.1. Colloidal masks-assisted chemical deposition

Combining microcontact printing with colloidal crystal masking, Xia *et al.* have developed a simple method – edge spreading lithography (ESL) – to generate mesoscopic structures on substrates [59]. As the name suggests, ESL utilizes the edges of masks – the perimeters of the footprint of particles on substrates – to define the features of resultant structures. The ESL procedure begins with formation of 2D colloidal crystals of silica beads on the surfaces of gold or silver thin films [59]. As shown in Fig. 9(left panel), typically, a planar polydimethylsiloxane (PDMS) stamp bearing a thin film of the ethanol solution of an alkanethiol was placed on a 2D silica colloidal crystal.

The thiol molecules were released from the stamp to the silica particle during contact and subsequently transferred to the substrate along the surfaces of silica particles, leading to a self-assembled monolayer (SAM) circling the footprint of each silica particle. The area of the thiol SAM could expand laterally via reactive spreading as long as the thiols were continuously supplies. Upon removal of the stamp and lift-off of the beads, the ring pattern was developed by wet etching with aqueous Fe^{3+}/thiourea using the patterned SAM as a resist [59]. Of importance is that ESL allows generation of the concentric rings of different alkanethiol SAMs by successive printing different thiol inks, and the removal of silica particle templates and selective etching yield concentric gold rings and the width of the rings were determined by the printing period (Fig. 9, right panel) [60].

Shin *et al.* have developed another way to integrate colloidal masking and contact printing, referred to contact area lithography (CAL), to directly generate periodic surface chemical patterns at the sub-100 nm scale [61, 62]. Different from ESL, CAL relies on self-assembly of octadecyltrichlorosilane (OTS). After a 2D colloidal crystal of silica was formed on silicon wafer, the SAM of OTS was homogeneously grown both on silica particles and the supporting silicon wafer via a sol-gel process. The removal of silica particles left behind a periodically arranged array of the openings in the OTS SAM with the same symmetry as that of 2D colloidal crystals. The openings were subsequently used as masks for growth of the ordered arrays of nanoparticles of such as titania or for selectively etching of the ordered arrays of silica cavities on the silicon wafer. In the case of growth of titania, nucleation is rather site-selective due to the significant difference in the surface energy between the growing and surrounding surfaces [63].

3.2.2. Colloidal masks-assisted physical deposition

In 1981 Fischer and Zingsheim have used 2D colloidal crystals as masks for contact imaging with visible light [22]. A year later Deckman and Dunsmuir have demonstrated the feasibility of using 2D colloidal crystals as masks for both physical deposition of materials and in turn patterning the surfaces of supporting substrates [63]. They have coined the term "Natural Lithography" to describe this process as "naturally" assembled single layers of latex particles were used as masks rather than lithographic masks. Later on they have expanded the capability of "Natural Lithography" and especially developed the RIE

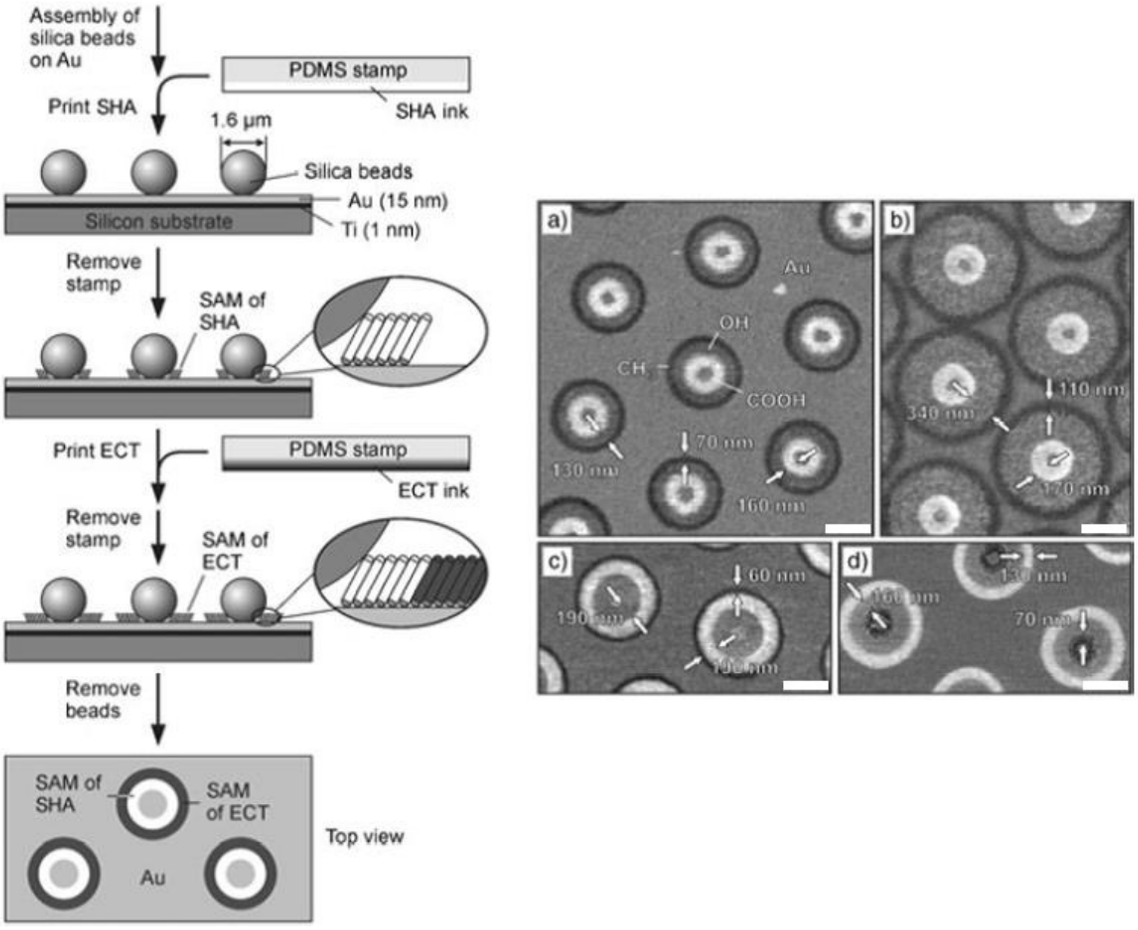

Figure 9. Left panel: Schematic illustration of the two-stepped ESL procedure used for side-by-side patterning of SHA and ECT monolayer rings on a gold substrate. Right panel. LFM images of concentric rings of carboxy- (bright), hydroxy-(gray), and methyl-terminated (dark) thiolate monolayers on gold. a) The rings were fabricated under the following conditions: 1 min for SHA, 1.5 min for HDDT, and 3 min for ECT. b) An increase in the printing times for HDDT and ECT to 3.5 and 4 min, respectively, resulted in wider rings for these two monolayers. c, d) The position of each monolayer in the concentric structure could be varied by changing the printing order. The pattern in (c) was generated by printing HDDT for 1.5 min, followed by printing of SHA and ECT for 3 min each. The sample shown in (d) was prepared by printing both ECT and HDDT for 1 min, and SHA for 2 min. All scale bars correspond to 500 nm. Reprinted with permission [60].

process for increasing the structural complexity of 2D colloidal crystal masks [48]. Since then the group of Van Duyne has devoted numerous efforts to develop patterning techniques using colloidal crystals as masks for metallic vapor deposition [23, 64-66]. In the context of nanoscience, they changed the name "Natural Lithography" to "Nanosphere Lithography" (NSL). Most important is that they have intensively investigated the plasmon resonance properties of metallic patterns obtained via NSL and their correlation with the feature morphology with the intent of developing high sensitive biosensors based on surface enhanced Raman spectroscopy (SERS) [67].

In a NSL procedure, a 2D colloidal crystal is used as masks for material deposition. The materials for physical deposition can be freely chosen without any limitations; commonly used are various metals such as gold and silver. The projection of the interstices between ordered

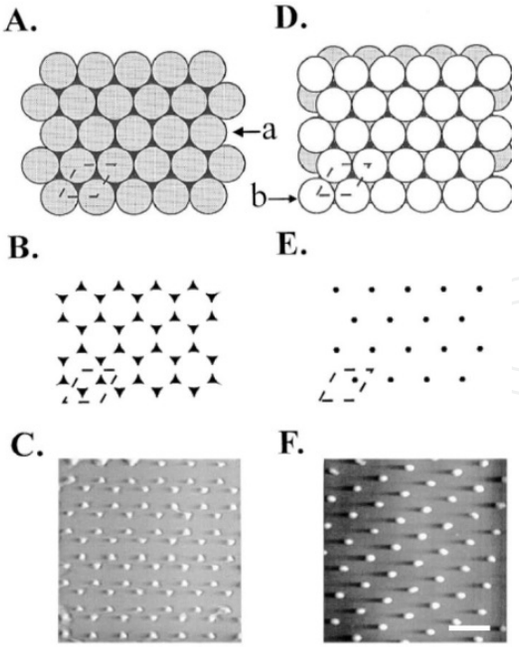

Figure 10. Schematic diagrams of single-layer (SL) and double-layer (DL) nanosphere masks and the corresponding periodic particle array (PPA) surfaces. (A) *a*(111) SL mask, dotted line represents the unit cell, *a* refers to the first layer nanosphere; (B) SL PPA, 2 particles per unit cell; (C) 1.7× 1.7 μm constant height AFM image of a SL PPA with M = Ag, S = mica, D = 264 nm, d_m = 22 nm, r_d = 0.2 nm s^{-1}. (D) *a*(111)*p*(1× 1)-*b* DL mask, dotted line represents the unit cell, *b*refers to the second layer nanosphere; (E) DL PPA, 1 particle per unit cell; (F) 2.0× 2.0 μm constant height AFM image of a DL PPA with M = Ag, S = mica, D = 264 nm, d_m = 22 nm, r_d = 0.2 nm s^{-1}. Scale bar: 300 nm. Reprinted with permission [23].

close-packed particles defines the shape of the nanodots deposited on substrates; the dots usually show a quasi-triangular shape and are arranged in a space group P6mm array due to the hexagonal packing of the colloidal crystal mask (Fig. 10a-c). Van Duyne *et al.* have extended colloidal crystal masking from single layer of hexagonally close packed particles to double layers [23]. Since the overlapping of the interstices between the upper and lower layers leads to a hexagonal array of quasi-hexagonal projection on a substrate, using double layer colloidal crystals as masks yields a hexagonal array of quasi-hexagonal nanodots (Fig. 10d-e).

In a general NSL procedure, the substrate to be patterned is positioned normal to the direction of material deposition. The in-plane shape of the nanodots and the spacing of the nearest-neighboring dots derived from NSL are dictated by the projection of the interstices of single or double layers of colloidal crystals on substrates. They can be tuned by varying the projection geometry of the interstices on substrates by titling the masks with respect to the incidence of the vapor beam for instance. This has inspired development of angle-resolved NSL (AR-NSL), pioneered by the group of Van Duyne [66].

In a AR-NSL process, the incidence angle of the propagation vector of the material deposition beam with respect to the normal direction of the colloidal mask (θ) and/or the azimuth angle of the propagation vector with respect to the nearest neighboring particles in the colloidal masks (ϕ) – the mask registry with respect to the vector of the material deposition beam – have been employed to reduce the size of the nanodots obtained and, at the same time, elongate

their triangular shape (Fig. 11). By rotating substrates, Giersig and coworkers have recently found that AR-NSL can generate much more complicate metallic nanostructures and they referred to this process as shadow NSL [43, 68, 69]. Zhang and Wang have recently demonstrated the feasibility of consecutively depositing two different metals, such as gold and silver, at two different incidence angles, to construct ordered binary arrays of gold and silver nanoparticles [70].Due to the rotation of the colloidal mask, shadow NSL relies in a process resolved by the azimuth angle (ϕ) of the incidence deposition beam rather than the incidence angle (θ).

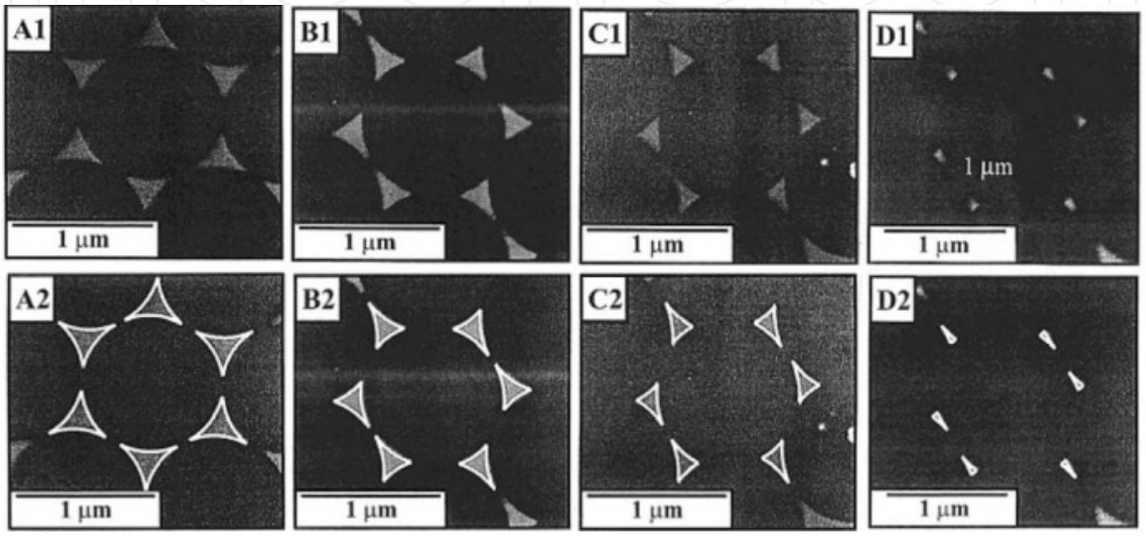

Figure 11. Field emission SEM images of AR NSL fabricated - gold nanodot arrays and images with simulated geometry superimposed, respectively. (A1, A2) θ = 108 °, ϕ = 288 °, (B1, B2) θ = 208 °, ϕ = 28 °, (C1, C2) θ = 268 °, ϕ = 168 °, and (D1, D2) θ = 408 °, ϕ = 28 °. All samples are Cr deposited onto Si (111) substrates. Images were collected at 40k magnification. θ is the incidence angle and ϕ the azimuth angle. Reprinted with permission [66].

The elegant extension of AR-NSL is to stepwise conduct physical vapor deposition of identical or different materials at the different incidence angles. The group of Van Duyne has succeeded in growth of surface patterning features composed of two triangular nanodots either overlapped or separated by two deposition steps at $\theta = 0^{o}$ and $\theta > 0^{o}$, respectively [65]. Giersig *et al.* have also developed a stepwise shadow NSL protocol to deposit different materials at different incidence angles when the colloidal masks were rotating and they have succeeded in encapsulation of the metallic structures to prevent them from oxidation [69].

Prior to physical vapor deposition, colloidal crystal masks can undergo RIE to reduce the sizes of the particles and widen the interstitial spaces, thus increasing the dimension of triangular nanodots obtained via NSL. Increasing the RIE time can turn close-packed colloidal crystal masks to non-close packed ones, which leads to thin films with hexagonally arranged pores [71, 72]. Wang *et al.* have recently integrated AR-NSL with the use of RIE-modified colloidal crystals as masks to diversify the structural complexity of the patterning feature derived from NSL from triangular (or deformed) nanodots to nanorods and nanowires [73]. Laterally arranging different nanowires into a periodic array with a defined alignment is hard to

implement by otherwise means, either conventional lithographic techniques or self-assembly techniques.

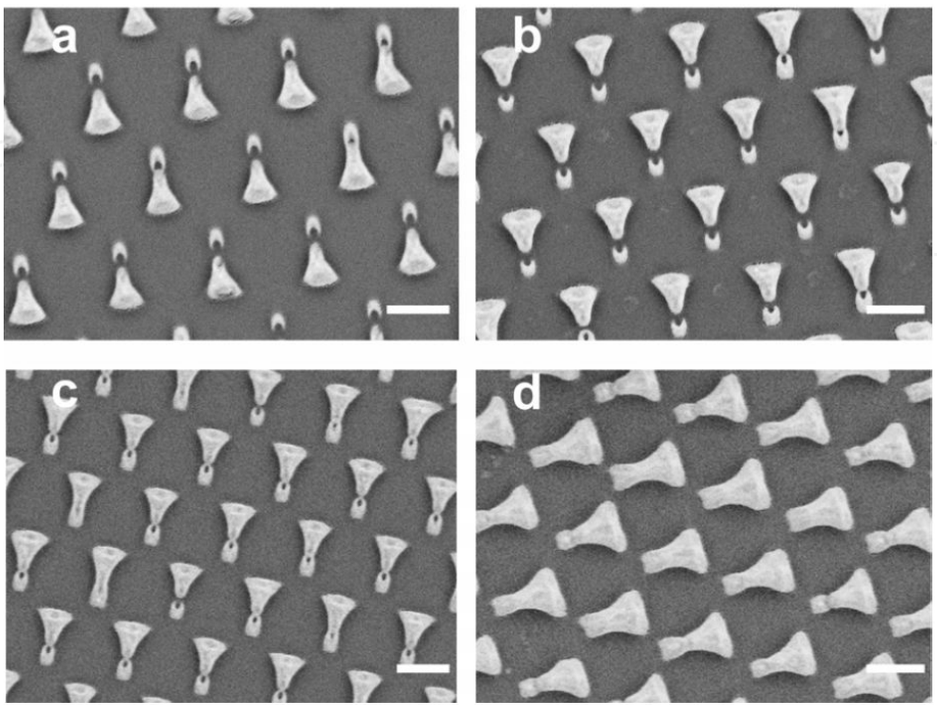

Figure 12. SEM pictures of hexagonally arranged Au nano-shuttlecocks obtained by using bilayers of hexagonal close-packed 925 nm PS spheres, etched by O_2-plasma for 10 (a), 20 (b), 25 (c), and 30 min (d), as masks for Au vapor deposition. The incidence angle of Au vapor flow was set as 15°. The scale bars are 500 nm. Reprinted with permission [74].

Wang *et al.* have recently extended the RIE process for modification of double layers of colloidal crystals for AR-NSL [74]. Using O_2 plasma etched bilayers of hexagonally packed particles as masks for gold deposition, highly ordered binary arrays of gold nanoparticles with varied shapes, for instance, with a shuttlecock-like shape composed of a small crescent-shaped nanoparticle and a big fan-shaped one, have been fabricated (Fig. 12). As compared to that of the corresponding bulk materials, the melting point of nanoparticles is much lower and especially more sensitive to the surface tension. Since the large curvature causes a high surface tension, the annealing of non-round nanoparticles may give rise to a retraction of their apexes, eventually generating a round shape [75]. Wang *et al.* have successfully transformed the shape of Au nanoparticles obtained from crescent-like or fan-shaped to round with a rather narrow distribution in terms of size and shape [74].

Dmitriev *et al.* have extended colloidal crystal masking from the use for material deposition to that for controlled etching and developed an interesting variant of NSL – hole-mask colloidal lithography (HCL) [76]. Different from conventional NSL, the essential new feature of HCL is that the substrate and the colloidal crystal mask are interspaced by a sacrificial layer. After physical vapor deposition, the removal of the colloidal mask leads to a thin film mask with nanoholes, which is known as "hole-mask". The hole-mask is subsequently used for vapor deposition and/or etching steps to further define a patterning feature on the substrate. HCL

includes a number of the advantages of NSL, such as large area coverage, high fabrication speed, independent control over feature size and spacing, and processing simplicity. It can be applied to a wide range of materials, including Au, Ag, Pd, Pt, SiO_2 etc.

Various colloidal spheres, organic and inorganic, can be produced that are exceedingly monodisperse in terms of size and shape. Nevertheless, their surfaces still remain chemically homogeneous or heterogeneous. Controlling the surface properties of colloidal particles is one of the oldest and, at the same time, the most vital topics in colloid science and physical chemistry. Patchy particles, i.e., particles with more than one patch or patches that are less than 50% of the total particle surface, should present the next generation of particles for assembly [77-79]. However, patterning the surface of colloidal particles with sizes of micrometers or submicrometers is a formidable challenge due to lack of the proper mask.

When 2D colloidal crystals are used as masks for physical vapor deposition, it is expected that only the upper surfaces of the colloidal particles, exposing directly to the vapor beam, will be coated with new materials, which leads to two spatially well-separated halves on the colloidal particles, coated and non-coated, with two distinct surface chemical functionalities [80, 81]. Such particles are usually referred to as Janus particles. By embedding a monomer of close-packed colloidal particles in a photoresist layer, Bao *et al.* have succeeded in tuning the surface areas of the colloidal particles exposing to the vapor beam during material deposition via etching the photoresist layer with O_2 plasma, thus leading to a good control of the domain sizes deposited on the particles [82]. When a monolayer of close-packed colloidal particles is constructed at the water/air interface or the wax/liquid interfaces, selective modification can be implemented in either of the two phases, leading to Janus particles [83, 84].

Wang *et al.* have pioneered the study of using the upper single layers of colloidal crystals as masks for the lower layer particles during physical vapor deposition [85]. Of importance is that the methodology reported by Wang *et al.* – using colloidal crystals for self-masking – is independent of the curvature and chemical composition of the surfaces (Fig. 13). By using O_2 plasma to etch colloidal crystal templates, mainly the top layer, and conducting physical vapor deposition at the non-zero incidence angle, Wang *et al.* have also demonstrated that the size and shape of the patterns obtained on the second layer particles show a pronounced dependence on the plasma etching time and the incidence angle [86]. Pawar and Kretzschmar have recently extended the concept of using colloidal crystal for self-masking for glancing angle deposition [87].

Wang *et al.* have recently employed the upper double layers as masks for patterning the particles in the third layers via physical deposition [88]. As a consequence, they have succeeded in stereo-decoration of colloidal particles with two, three, four, or five nanodots. The number of dots per sphere is dependent on the crystalline structure of the colloidal crystal masks, the plasma etching time, and the incidence angle. The nanodots decorated on particles are arranged in a linear, trigonal, tetrahedral, or right-pyramidal fashion, which provides the nanoscale analogues of sp, sp2, sp3 sphybridized atomic orbitals of carbon. The Au nanodots obtained on microspheres, therefore, can be recruited as the bonding site to dictate the integration of the spheres, thus paving a new way of colloidal self-assembly – colloidal valent chemistry of spheres [89] – to create hierarchical and complicated "supraparticles" [77].

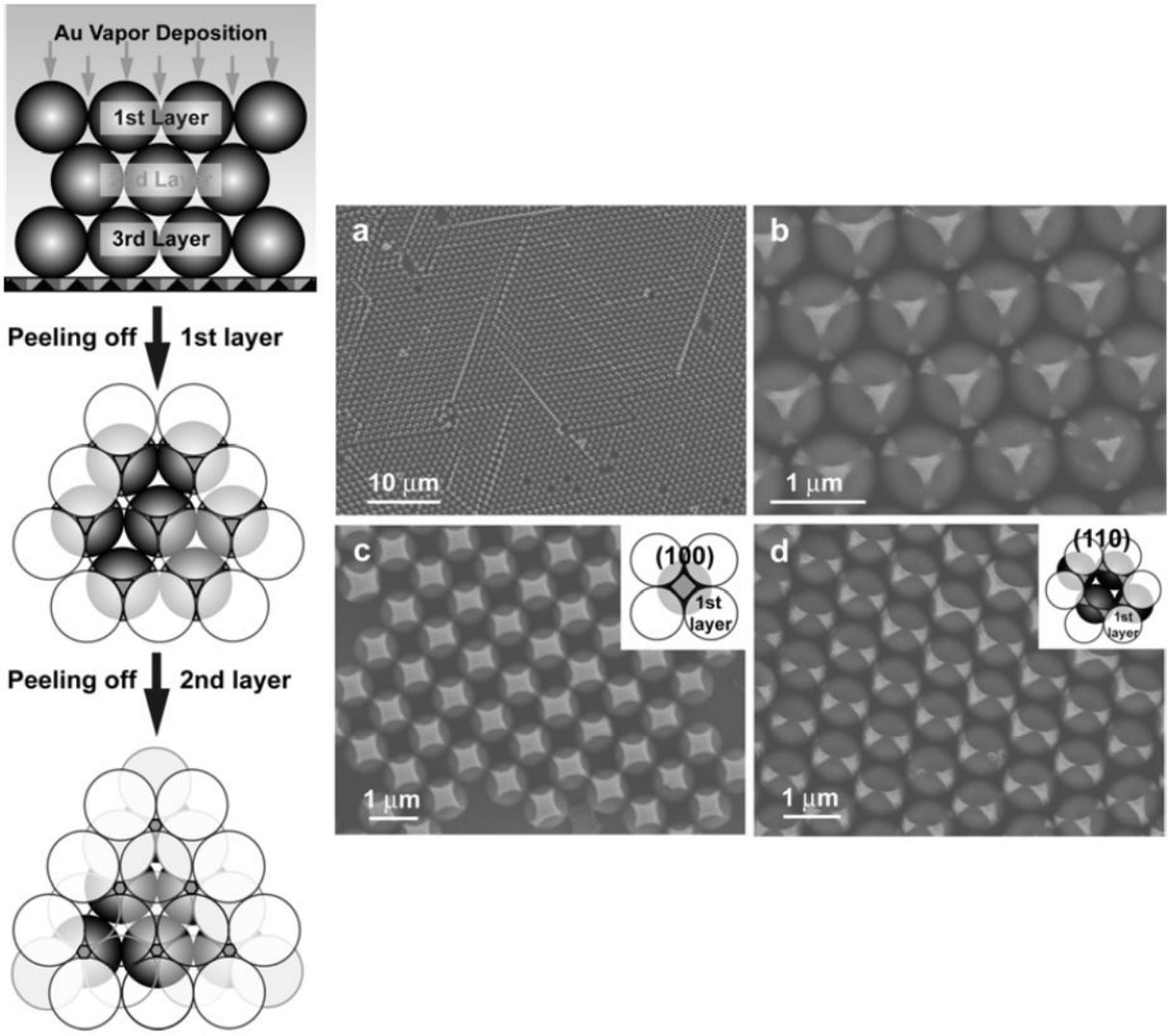

Figure 13. Left panel: Schematic illustration of the procedure to create colloidal spheres with Au-patterned surfaces by the combination of Au vapor deposition and using the top mono- or bilayers of colloidal crystals with (111) facets parallel to the substrates as masks. Right panel: Low (a) and high magnification scanning electron microscope (SEM) picture of 925 nm polystyrene spheres with Au patterned surfaces generated by templating the top monolayers of colloidal crystals with (111) (b) (100) (c) and (110) (d) facets parallel to the substrates. Reprinted with permission [85]

3.2.3. Extension of colloidal lithography

One extension of NSL is to use the surface patterns obtained as templates to grow nanostructures of a variety of materials via bottom-up self-assembly. Mulvaney's group has grown monolayer and multilayer films of semiconductor quantum dots on surface patterns derived from NSL, leading to nanostructured luminescent thin films [90, 91]. Valsesia *et al.* have used ordered arrays of polyacrylic acid domes derived via NSL to selectively couple with bovine serum albumin [55]. Using NSL-derived surface patterns as templates to grow proteins, Sutherland *et al* have found that the surface topography enhances the binding selectivity of fibrinogens to platelets [92].

http://dx.doi.org/10.5772/56576

The second extension is to use NSL-derived surface patterns as etching masks to create surface topography. Chen *et al.* have fabricated silicon nanopillar arrays with diameters as small as 40 nm and aspect ratios as high as seven [93]. The size and shape of the nanopillars can be controlled by the size and shape of the sputtered aluminum masks, which are again determined by the feature size of the colloidal mask and the number of the colloidal layers. Nanopillars with different shapes can also be fabricated by adjusting the RIE conditions such as the gas species, bias voltage, and exposure duration for an aluminum mask with a given shape. As-prepared nanopillar arrays can be utilized for imprinting a layer of PMMA above its glass transition temperature [94]. Similarly, Weekes *et al.* have fabricated ordered arrays of cobalt nanodots for patterned magnetic media [95]. By introducing intermediary layers of SiO_2 between colloidal crystal masks and substrates, this etching strategy can be applied to a wide range of materials without much concern for the surface hydrophilicity of the targeted substrates. Using the similar protocol, large-area ordered arrays of 512 nm pitch hole, with vertical and smooth sidewalls, has been successfully formed on GaAs substrates [96].

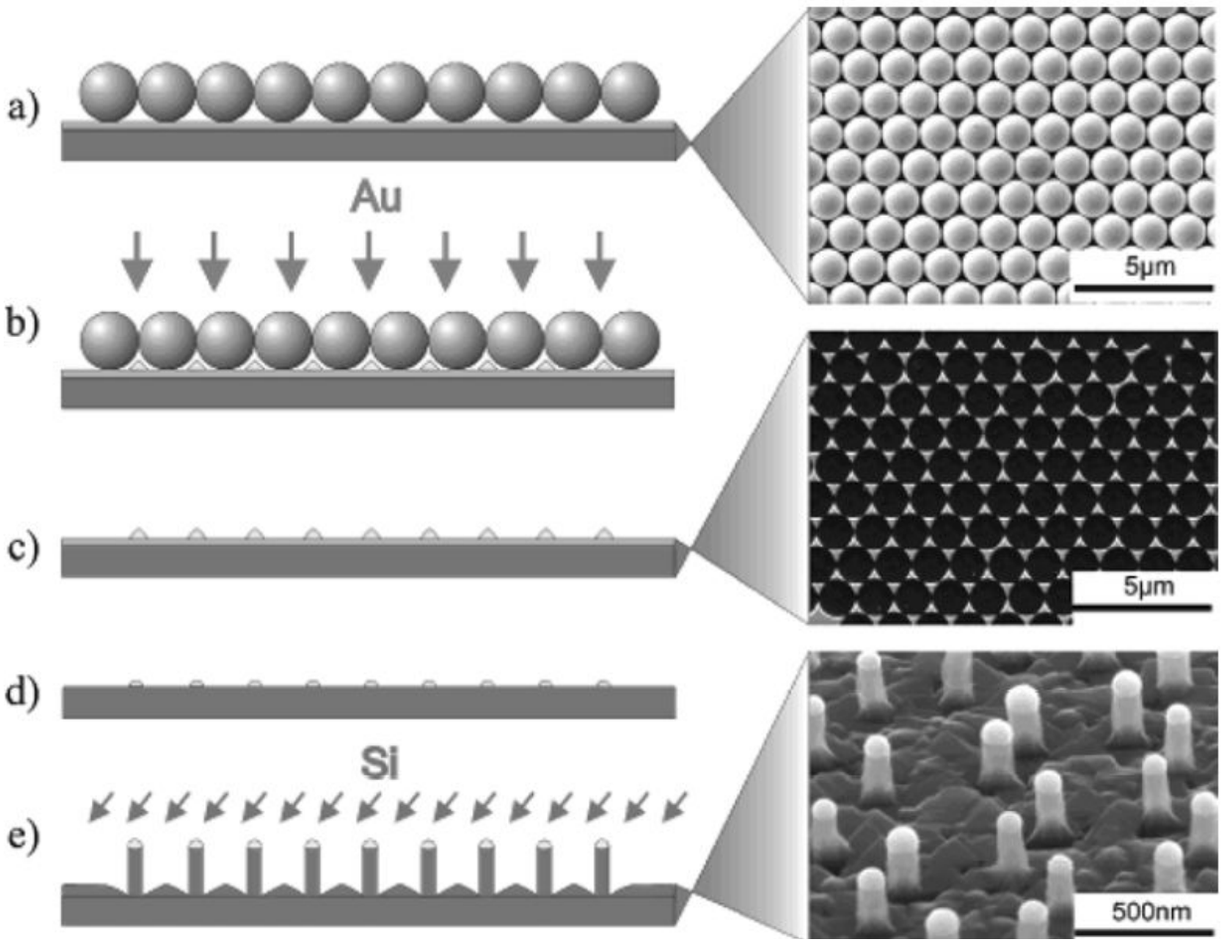

Figure 14. Steps of Si nanowire fabrication. NSL: (a) deposition of a mask of polystyrene particles (b) deposition of gold by thermal evaporation, (c) removal of the spheres, (d) thermal annealing and cleaning step to remove the oxide layer, and (e) Si deposition and growth of nanowires by MBE. (Right) corresponding SEM micrographs of wafers at different steps. Reprinted with permission [100].

The third extension is to use NSL-derived surface patterns to template or catalyze the growth of other functional materials. Zhou *et al.* have successfully used the ordered arrays of gold nanodots derived from NSL as seeds to highly aligned single-walled carbon nanotubes laid on quartz and sapphire substrates [97]. This method has great potential to produce carbon nanotube arrays with simultaneous control over the nanotube orientation, position, density, diameter, and even chirality, which may work as building blocks for future nanoelectronics and ultra-high-speed electronics [98]. Wang *et al.* have used gold nanodot arrays as seeds for hexagonally arranged arrays of zinc oxide nanorods aligned perpendicular to the substrates [99]. Similarly Fuhrmann *et al.* have obtained ordered arrays of Si nanorods by using the gold nanodots as seeds for molecular beam epitaxy (Fig. 14) [100]. Similarly, discretely ordered arrays of organic light-emitting nanodiode (OLED) have been fabricated based on NSL-derived surface patterns [101].

4. Applications

4.1. Optical properties

Surface patterns derived from CL, especially NSL, are usually made up of metals such as gold and silver. Noble metal nanostructure arrays have pronounced surface plasmon resonance, which results from incident electromagnetic radiation exciting coherent oscillations of conduction electrons near a metal-dielectric interface [102]. Giessen and co-workers introduced an angle-controlled colloidal lithography as a fast and low-cost fabrication technique for large-area periodic plasmonic oligomers with complex shape and tunable geometry parameters, and investigated the optical properties and found highly modulated plasmon modes in oligomers with triangular building blocks. Fundamental modes, higher-order modes, as well as Fano resonances due to coupling between bright and dark modes within the same complex structure are present, depending on polarization and structure geometry. This process is well-suited for mass fabrication of novel large-area plasmonic sensing devices and nanoantennas (Fig. 15) [103].

One of the straightforward technical applications of CL is to use as highly sensitive biosensors relied on the localized-surface plasmon resonance (LSPR) of metallic nanostructures [67]. The LSPR of metallic nanostructures composed of gold rings [104] and disks [105], obtained via NSL has been studied. It is found that the LSPR can be tuned by varying either the diameter of the disks at a constant disk height or the ring thickness. The shape-dependent red shift originates from the electromagnetic coupling between the inner and outer ring surfaces, which leads to energy shifts and splitting of degenerate modes [106]. NSL has been also used to create nanocaps and nanocups; their LSPR behavior has been studied [107]. Lee *et al.* have generated gold crescent moon structures with a sub-10 nm sharp edge via NSL, which exhibit a very strong SERS [108].

http://dx.doi.org/10.5772/56576

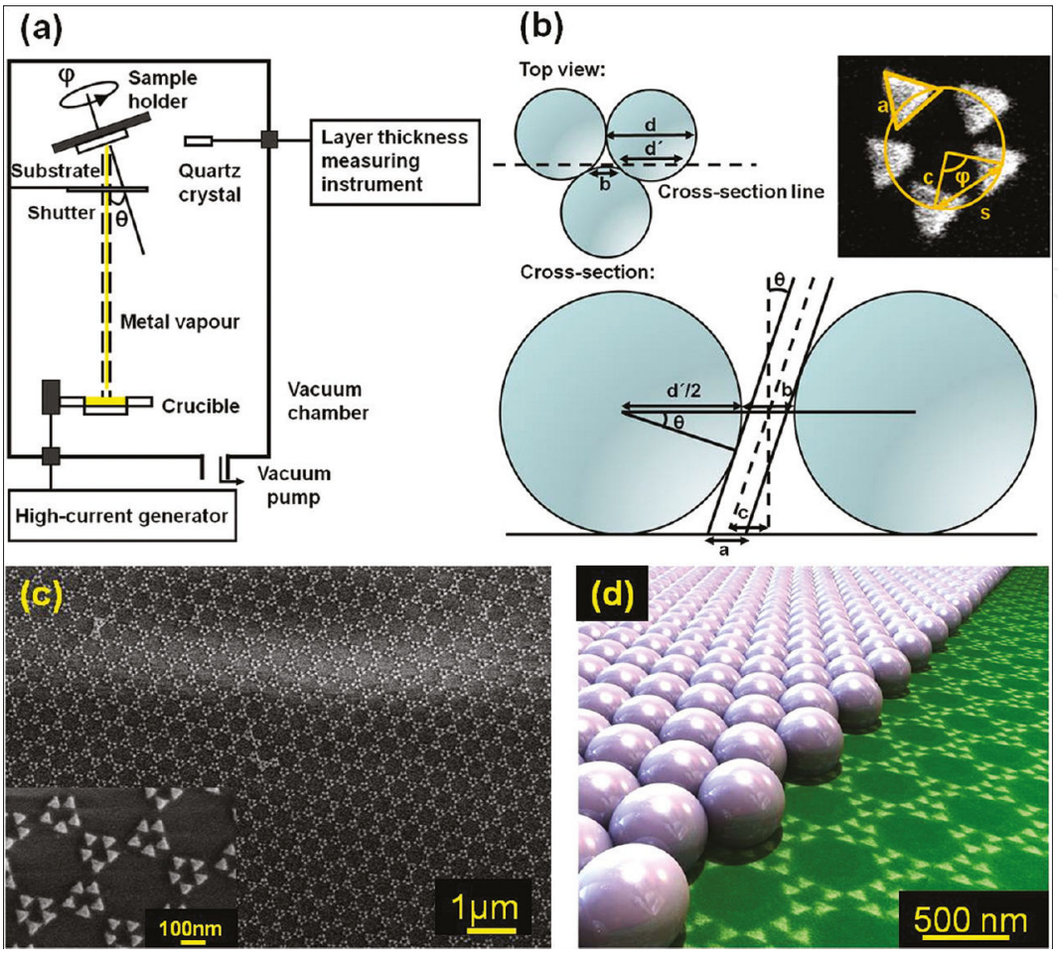

Figure 15. Fabrication of oligomers with triangular building blocks. (a) Schematic diagram of the evaporation setup. (b)Simplified geometrical model for symmetric pentamer fabrication. Top left: top view. Bottom: side view at cross section line as indicated in top view. Top right: geometrical parameters. (c) Scanning electron microscopy (SEM) images of the large are asymmetric pentamers. The gap size is as small as 20 nm. (d) Artistic view of our fabrication scheme, using a real SEM image of a symmetric pentamer. The transmittance spectrum of the sample using a large-area optical beam diameter. Reprinted by permission of [103].

Light trapping across a wide band of frequencies is important for applications such as solar cells and photo detectors. Yao Y. and Yao J. *et al.* demonstrated a new approach based on colloidal lithography to light management by forming whispering-gallery resonant modes inside a spherical nanoshell structure. A broadband absorption enhancement across a large range of incident angles was observed. The absorption of a single layer of 50-nm-thick spherical nanoshells is equivalent to a 1-µm-thick planar nc-Si film. This light-trapping structure could enable the manufacturing of high-throughput ultra-thin film absorbers in a variety of material systems that demand shorter deposition time, less material usage and transferability to flexible substrates. [109]

4.2. Wettability

The wettability of solid surfaces is a significant property depending on both chemical compositions and the surface structure. A great number of ordered arrays generated through simple

or modified colloidal lithography could induce different wettabilities. Recently, Koshizaki and co-workers fabricated vertically ordered Co_3O_4 hierarchical nanorod arrays using pulsed laser deposition (PLD) onto colloidal crystal masks followed by an annealing process, and the as-prepared Co_3O_4 nanorod arrays demonstrated stable superhydrophilicity without UV irradiation even after half a year owing to the improved roughness of the hierarchical structure and the abundant OH− groups induced by the PLD and annealing processes.

4.3. Other applications

Besides the exploitation of CL and the patterns obtained thereof in LSPR-assisted sensing, the magnetic properties of CL-derived nanostructures gain increasing attention. In general, nanoscale magnetic materials often exhibit superparamagnetic behavior. Moreover, an ordered nanostructure of magnetic materials is required for investigation of the mesoscopic effects induced by the confinement of magnetic materials in nanoscale domains [111]. Since magnetic properties are strongly dependent on the domain size and the distance between domains, Weekes *et al.* have created ordered arrays of isolated magnetic nanodots via NSL [95]. The coercivity and switching width of the isolated nanodot arrays are enhanced as compared to those of continuous magnetic films. Well-organized arrays of magnetic nanorings over a large area have been prepared via NSL and they show a stable vortex state due to the absence of a destabilizing vortex core, which should hold promise in vertical magnetic random access memories [112, 113]. Albrecht *et al.* have found that Co/Pd multilayers on a colloid surface exhibited a pronounced magnetic anisotropy [114].

What's more, a core question in materials science is how to encode non-trivial organized structures within simple building blocks. A recent report from this laboratory described methods for functionalizing latex spheres to make them hydrophobic at their poles, leading to the directed self-assembly of a kagome lattice pattern in which each sphere was coordinated with four neighbors, two at each pole. Granick and co-workers developed methods for functionalizing micrometer-sized colloidal spheres with three or more zones of chemical functionality through colloidal lithography, literally combining double-sided angle-resolved physical deposition and controllable chemical etching. These synthesis methods allowed targeting of various lattice structures whose bonding between neighboring particles in liquid suspension was visualized in situ by optical microscopy [115,116].

5. Summary

The recent development of CL, especially the integration of etching the colloidal mask, altering the incidence angle, and stepwise and regularly changing the mask registry, leads to a powerful nanochemical patterning tool with low cost in capital and operation, high throughput, and ease to be adopted on various planar and curved surfaces and even on microparticles. Different from conventional mask-assisted lithographic processes in which the mask design and production usually remain a challenge for scaling down the feature size and diversifying the feature shape, CL embodies a simple way for masking – self-assembly of monodisperse

microspheres on a targeted substrate. The feature size can easily shrink below 100 nm by reducing the diameter of the microspheres used according to the simple correlation between the interstice size and the sphere diameter. The feature shape can be easily diversified by the crystalline structure of a colloidal crystal mask, the time of anisotropic etching of the mask, the incidence angle of vapor beam and the mask registry (the azimuth angle of vapor beam). Currently, CL allows fabrication of very complicated 2D and 3D nanostructured features, such as multiplex nanostructures with a clear-cut lateral and vertical heterogeneity. A number of new nanostructures are hard to be implemented, or cannot be in some cases, by conventional lithographic techniques. As such, CL provides a nanochemical and complementary tool of conventional and fully top-down lithographic techniques, and thus holds immense promise in surface patterning.

However, CL is still in a very early stage of development. Despite the great progress in colloidal crystallization it still remains a formidable challenge to create a defect-free single crystal with a defined crystalline face. The presence of defects dramatically reduces the patterning precision of CL. For instance, the random orientation of polycrystalline crystalline domains in a colloidal mask is a disaster for collimating the mask registry. In this aspect, template-assisted epitaxy for colloidal crystallization is promising as it allows growth of colloidal crystals with defined packing structure and orientation. Since a patterned substrate is necessitated for the colloidal epitaxy, its applicability for patterning is limited. How to transfer a colloidal crystal derived from this colloidal epitaxy onto different substrates without deterioration of the crystal quality should be an ensuing task for CL. Besides, fabrication of large area monolayer of periodically close-packed microspheres with sizes smaller than 100 nm remains highly challenging, which brings a technical problem to reduce the feature size below 10 nm via CL. In a CL patterning process, furthermore, the feature size and the interspace size between the features cannot be separately manipulate, as they both are directly proportional with the sphere size in a colloidal mask, which largely limit the patterning capability of CL.

Author details

Ye Yu and Gang Zhang*

*Address all correspondence to: gang@jlu.edu.cn

State Key Lab of Supramolecular Structure and Materials, College of Chemistry, Jilin University, Changchun, China

References

[1] D. Wang, H. Möhwald, Template-directed colloidal self-assembly – the route to 'top-down' nanochemical engineering, *J. Mater. Chem.* 2004, *14*, 459-468.

[2] Y. Xia, B. Gates, Y. Yin, Y. Lu, Monodisperse colloidal particles: old materials with new applications, *Adv. Mater.* 2000, *12*, 693-713.

[3] M. E. Leunissen, C. G. Christova, A-P, Hynninen, C. P. Royall, A. I. Campbell, A. Imhof, M. Dijkstra, R. van Roij, A. van Blaaderen, Ionic colloidal crystals of oppositely charged particles, *Nature* 2005, *437*, 235-240.

[4] R. Mayoral, J. Requena, J. S. Moya, C. López, A. Cintas, H. Miguez, F. Meseguer, L. Vazquez, M. Holgado, A. Blanco, 3D long-range ordering in and SiO_2 submicrometer-sphere sintered superstructure, *Adv. Mater.* 1997, *9*, 257-260.

[5] H. Miguez, F. Meseguer, C. López, A. Mifsud, J. S. Moya, L. Vazquez, Evidence of FCC crystallization of SiO_2 nanospheres, *Langmuir* 1997, *13*, 6009-6011.

[6] H. Migurez, C. López, F. Meseguer, A. Blanco, L. Vazquez, R. Mayoral, M. Ocafia, V. Fornes, A. Mifsud, Photonic crystal properties of packed submicrometric SiO_2, *Appl. Phys. Lett.* 1997, *71*, 1148-1150.

[7] N. D. Denkov, O. D. Velev, P. A. Kralchevsky, I. B. Invanov, H. Yoshimura, K. Nagayama, Mechanism of formation of 2D crystals from latex-particles on substrates, *Langmiur*1992, *8*, 3183-3190.

[8] R. Micheletto, H. Fukuda, M. Ohtsu, A simple method for the production of a 2D ordered array of small latex-particles, *Langmuir*, 1995, *11*, 3333-3336.

[9] A. S. Dimitrov, K. Nagayama, Continuous convective assembling of fine particles into 2D arrays on solid surfaces, *Langmuir* 1996, *12*, 1303-1311.

[10] P. Jiang, J. F. Bertone, K. S. Hwang, V. L. Colvin, Single-crystal colloidal multilayers of controlled thickness, *Chem. Mater.* 1999, *11*, 2132-2140.

[11] Z. –Z., Gu, A. Fujishima, O. Sato, Fabrication of high-quality opal films with controllable thickness, *Chem. Mater.* 2002, *14*, 760-765.

[12] Z. Zhou, X. S. Zhao, Flow-controlled vertical deposition method for the fabrication of photonic crystals, *Langmuir* 2004, *20*, 1524-1526.

[13] S. Wong, V. Kitaev, G. A. Ozin, Colloidal crystals films: advances in universality and perfection, *J. Am. Chem. Soc.* 2003, *125*, 15589-15598.

[14] X. Chen, Z. Chen, N. Fu, G. Lu, B. Yang, Versatile nanopatterned surfaces generated via 3D colloidal crystals, *Adv. Mater*. 2003, *15*, 1413-1417.

[15] Y. W. Chung, I. C. Leu, J. H. Lee, M.H. Hon, Influence of humidity on the fabrication of high-quality colloidal crystals via a capillary-enhanced process, *Langmuir* 2006, *22*, 6454-6460.

[16] M. H. Kim, S. H. Im, O. O. Park, Rapid fabrication of two- and three-dimensional colloidal crystal films via confined convective assembly, *Adv. Funct. Mater.* 2005, *15*, 1329-1335.

[17] Z. Cheng, W. B. Russel, P. M. Chaikin, Controlled growth of hard-sphere colloidal crystals, *Nature* 1999, *401*, 893-895.

[18] S. H. Im, M. H. Kim, O. O. Park, Thickness control of colloidal crystals with a substrate dipped at a tilted angle into a colloidal suspension, *Chem. Mater*. 2003, *15*, 1797-1802.

[19] V. Kitaev, G. A. Ozin, Self-assembled surface patterns of binary colloidal crystals, *Adv. Mater*. 2003, *15*, 75-78.

[20] K. P. Velikov, C. G. Christova, R. P. A. Dullens, A. van Blaaderen, Layer-by-layer growth of binary colloidal crystals, *Science* 2002, *296*, 106-109.

[21] M. H. Kim, S. H. Im, O. O. Park, Fabrication and structural analysis of binary colloidal crystals with 2D superlattices, *Adv. Mater*. 2005, *17*, 2501-2505.

[22] U. C. Fischer, H. P. Zingsheim, Submicroscopic pattern replication with visible light, *J. Vac. Sci. Technol.* 1981, *19*, 881-885.

[23] J. C. Hulteen, R. P. van Duyne, Nanosphere lithography-a materials general fabrication process for periodic particle array surfaces, *J. Vac. Sci. Technol. A*. 1995, *13*, 1553-1558.

[24] T. J. Rehg, B. G. Higgins, Spin coating of colloidal suspensions, *AIChE*1992, *38*, 489-501.

[25] P. Jiang, M. J. McFarland, Large-scale fabrication of wafer-size colloidal crystals, macroporous polymers and nanocomposites by spin-coating, *J. Am. Chem. Soc.* 2004, *126*, 13778-13786.

[26] P. Jiang, M. J. McFarland, Wafer-scale periodic nanoholes arrays templated from 2D non-close-packed colloidal crystals, *J. Am. Chem. Soc.* 2005, *127*, 3710-3711.

[27] D. Wang, H. Möhwald, Rapid fabrication of binary colloidal crystals by stepwise spin-coating. *Adv. Mater.* 2004, *16*, 244-247.

[28] A. Ulman, An introduction to ultrathin organic films: from Langmuir-Blodgett to self-assembly, *Academic Press*, Boston, 1991.

[29] B. P. Binks, Particles as surfactants-similarities and differences. *Current Opinion in Colloid & Interface Science* 2002, *7*, 21-41.

[30] P. Pieranski, Two dimensional interfacial colloidal crystals. *Phys. Rev. Lett.* 1980, *45*, 569-572.

[31] S. H. Im, Y. T. Lim, D. J. Suh, O. O. Park, 3D self-assembly of colloids at a water-air interface: A novel technique for the fabrication of photonic bandgap crystals. *Adv. Mater*. 2002, *14*, 1367-1369.

[32] M. Kondo, K. Shinozaki, I. Bergström, N. Mizutani, Preparation of colloidal monolayers of alkoxylated silica particles at the air-liquid interface. *Langmuir* 1995, *11*, 394-397.

[33] K. -U. Fulda, B. Tieke, Langmuir films of monodisperse 0.5μm spherical polymer particles with a hydrophobic core and a hydrophilic shell. *Adv. Mater.* 1994, *6*, 288-290.

[34] B. van Duffel, R. H. A. Ras, F. C. De Schryver, R. A. Schoonheydt, Langmuir-Blodgett depostion and optical diffraction of two dimensional opal. *J. Mater. Chem.* 2001, *11*, 3333-3336.

[35] S. Reculusa, S. Ravaine, Synthesis of colloidal crystals of controllable thickness through the Langmuir-Blodgett technique. *Chem. Mater.* 2003, *15*, 598-605.

[36] N. Vogel, L. de Viguerie, U. Jonas, C. K. Weiss, K. Landfester, Wafer-scale fabrication of ordered binary colloidal monolayers with adjustable stoichiometries. *Adv. Funct. Mater.*2011, *21*, 3064-3073.

[37] L. M. Goldenberg, J. Wagner, J. Stumpe, B-R. Paulke, E. Grnitz, Simple method for the preparation of colloidal particle monolayers at the water/alkane interface. *Langmuir* 2002, *18*, 5627-5629.

[38] S. Reynaert, P. Moldenaers, J. Vermant, Control over colloidal aggregation in monolayers of latex particles at the oil-water interface. *Langmuir* 2006, *22*, 4936-4945.

[39] K. P. Velikov, F. Durst. O. D. Velev, Direct observation of the dynamics of latex particles confined inside thinning water-air films. *Langmuir* 1998, *14*, 1148-1155.

[40] Z-Z Gu, D. Wang, H. Möhwald, Self-assembly of microspheres at the air/water/air interface into free-standing colloidal crystal films. *Soft Matter* 2007, *3*, 68-70.

[41] B. Griesebock, M. Egen, R. Zental, Large photonic films by crystallization on fluid substrates. *Chem. Mater.* 2002, *14,* 4023-4025.

[42] P. Hanarp, M. Kall, D. S. Sutherland, Optical properties of short range ordered arrays of nanometer gold disks prepared by colloidal lithography. *J. Phys. Chem. B* 2003, *107*, 5768-5772.

[43] A. Kosiorek, W. Kandulski, H. Glaczynska, M. Giersig, Fabrication of nanoscale rings, dots, and rods by combining shadow nanosphere lithography and annealed polystyrene nanosphere masks. *Small* 2005, *1*, 439-444.

[44] J. H. Moon, W.-S. Kim, J.-W. Ha, S. G. Jang, S.-M. Yang, J. K. Park, Colloidal lithography with crosslinkable particles: Fabrication of hierarchical nanopore arrays, *Chem. Commun.* 2005, *32*, 4107-4109.

[45] J. J. Peninkhof, C. Graf, T. van Dillen, A. M. Vredenberg, A. van Blaaderen, A. Polman, Angle-dependent extinction of anisotropic silica/Au core/shell colloids made via ion irradiation. *Adv. Mater.* 2005, *17*, 1484-1488.

[46] D. L. J. Vossen, D. Fific, J. Penninkhof, T. Van Dillen, A. Polman, A. Van Blaaderen, Combined optical tweezers/ion beam technique to tune colloidal masks for nanolithography, *Nano Lett.* 2005, *5*, 1175-1179.

[47] J. D. Forster, J. Park, M. Mittal, H. Noh, C. F. Schreck, C. S. O'Hern, H. Cao, E. M. Furst, E. R. Dufresne, Assembly of Optical-Scale Dumbbells into Dense Photonic Crystals, ACS Nano 2011, 5, 6695-6700.

[48] H. W. Deckmann, J. H. Dunsmuir, Applications of surface textures produced with natural lithography. *J. Vac. Sci. Technol. B* 1983, *1*, 1109-1112.

[49] D.-G. Choi, H. K. Yu, S. G. Jang, S.-M. Yang, Colloidal lithographic nanopatterning via reactive ion etching. *J. Am. Chem. Soc.* 2004, *126*, 7019-7025.

[50] S.-M. Yang, S. G. Jang, D.-G. Choi, S. Kim, H. K. Yu, Nanomachining by colloidal lithography. *Small* 2006, *2*, 458-475.

[51] D.-G. Choi, S. G. Jang, S. Kim, E. Lee, C.-S. Han, S.-M. Yang, Multifaceted and nanobored particle arrays sculpted using colloidal lithography. *Adv. Funct. Mater.* 2006, *16*, 33-40.

[52] Y. Zheng, Y. Wang, S. Wang, C. H. A. Huan, Fabrication of nonspherical colloidal particles via reactive ion etching of surface-patterned colloidal crystals. *Colloid Surf. A* 2006, *277*, 27-36.

[53] C. L. Cheung, R. J. Nikolić, C. E. Reinhardt, T. F. Wang, Fabrication of nanopillars by nanosphere lithography. *Nanotechnology* 2006, *17*, 1339-1343.

[54] B. J.-Y. Tan, C.-H. Sow, K.-Y. Lim, F.-C. Cheong, G.-L. Chong, A. T.-S. Wee, C.-K. Ong, Fabrication of a two-dimensional periodic non-close-packed array of polystyrene particles. *J. Phys. Chem. B* 2004, *108*, 18575-18579.

[55] A. Valsesia, P. Colpo, M. M. Silvan, T. Meziani, G. Ceccone, F. Rossi, Fabrication of nanostructured polymeric surfaces for biosensing devices. *Nano Lett.* 2004, *4*, 1047-1050.

[56] B. Wang, W. Zhao, A. Chen, S.-J. Chua, Formation of nanoimprintingmould through use of nanosphere lithography. *J. Crystal Growth* 2006, *288*, 200-204.

[57] Z. Huang, H. Fang, J. Zhu, Fabrication of silicon nanowire arrays with controlled diameter, length, and density. *Adv. Mater.* 2007, *19*, 744-748.

[58] B. J. Y. Tan, C. H. Sow, T. S. Koh, K. C. Chin, A. T. S. Wee, C. K. Ong, Fabrication of size-tunable gold nanoparticles array with nanosphere lithography, reactive ion etching, and thermal annealing. *J. Phys. Chem. B* 2005, *109*, 11100-11109.

[59] J. M. McLellan, M. Geissler, Y. Xia, Edge spreading lithography and its application to the fabrication of mesoscopic gold and silver rings. *J. Am. Chem. Soc.* 2004, *126*, 10830-10831.

[60] M. Geissler, J. M. McLellan, J. Chen, Y. Xia, Side-by-side patterning of multiple alkanethiolate monolayers on gold by edge-spreading lithography. *Angew. Chem. Int. Ed.* 2005, *44*, 3596-3600.

[61] C. Bae, H. Shin, J. Moon, M. M. Sung, Contact area lithography (CAL): A new approach to direct formation of nanometric chemical patterns. *Chem. Mater.* 2006, *18*, 1085-1088.

[62] C. Bae, J. Moon, H. Shin, J. Kim, M. M. Sung, Fabrication of monodisperse asymmetric colloidal clusters by using contact area lithography (CAL). *J. Am. Chem. Soc.*2007, *129*, 14232-14239.

[63] H. W. Deckmann, J. H. Dunsmuir, Natural lithography. *Appl. Phys. Lett.* 1982, *41*, 377-379.

[64] J. C. Hulteen, D. A. Treichel, M. T. Smith, M. L. Duval, T. R. Jensen, R. P. Van Duyene, Nanosphere lithography: size-tunable silver nanoparticle and surface cluster arrays. *J. Phys. Chem. B* 1999, *103*, 3854-3863.

[65] C. L. Haynes, R. P. Van Duyne, Nanosphere lithography: A versatile nanofabrication tool for studies of size-dependent nanoparticle optics. *J. Phys. Chem. B* 2001, *105*, 5599-5611.

[66] C. L. Haynes, A. D. McFarland, M. T. Smith, J. C. Hulteen, R. P. Van Duyne, Angle-resolved nanosphere lithography: Manipulation of nanoparticle size, shape, and interparticle spacing. *J. Phys. Chem. B* 2002, *106*, 1898-1902.

[67] A. Willets, R. P. Van Duyne, Localized surface plasmon resonance spectroscopy and sension. *Annu. Rev. Phys. Chem.* 2007, *58*, 267-297.

[68] M. Giersig, M. Hilgendorff, Magnetic nanoparticle superstructures. *Eur. J. Inorg. Chem.* 2005, 3571-3583.

[69] A. Kosiorek, W. Kandulski, P. Chudzinski, K. Kempa, M. Giersig, Shadow nanosphere lithography: Simulation and experiment. *Nano Lett.* 2004, *4*, 1359-1363.

[70] G. Zhang, D. Wang, Fabrication of heterogeneous binary arrays of nanoparticles via colloidal lithography. *J. Am. Chem. Soc.* 2008, *130*, 5616-5617.

[71] S. M. Weekes, F. Y. Ogrin, Torque studies of large-area Co arrays fabricated by etched nanosphere lithography. *J. Appl. Phys.* 2005, *97*, 10J503.

[72] D.-G. Choi, S. Kim, S. G. Jang, S.-M. Yang, J.-R. Jeong, S.-C. Shin, Nanopatterned magnetic metal via colloidal lithography with reactive ion etching. *Chem. Mater.* 2004, *16*, 4208-4211.

[73] G. Zhang, D. Wang, H. Möhwald, Fabrication of multiplex quasi-three-dimensional grids of one-dimensional nanostructures via stepwise colloidal lithography. *Nano Lett.* 2007, *7*, 3410-3413.

[74] G. Zhang, D. Wang, H. Möhwald, Ordered binary arrays of Au nanoparticles derived from colloidal lithography. *Nano Lett.* 2007, *7*, 127-132.

[75] A. Habenicht, M. Olapinski, F. Burmeister, P. Leiderer, J. Boneberg, Jumping nanodroplets. *Science,* 2005, *309,* 2043-2045.

[76] H. Fredriksson, Y. Alaverdyan, A. Dmitriev, C. Langhammer, D. S. Sutherland, M. Zäch, B. Kasemo, Hole-mask colloidal lithography. *Adv. Mater.* 2007, *19*, 4297-4302.

[77] E. W. Edwards, D. Wang, H. Möhwald, Hierarchical organization of colloidal particles: from colloidal crystallization to supraparticle chemistry. *Macromol. Chem. Phys.* 2007, *208,* 439-445.

[78] H. Zhang, E. W. Edwards, D. Wang, H. Möhwald, Directing the self-assembly of nanocrystals beyond colloidal crystallization. *Phys. Chem. Chem. Phys.* 2006, *8,* 3288-3299.

[79] S. C. Glotzer, M. J. Solomon, Anisotropy of building blocks and their assembly into complex structures. *Nature Mater.* 2007, *6,* 557-562.

[80] K. Fujimoto, K. Nakahama, M. Shidara, H. Kawaguchi, Preparation of unsymmetrical microspheres at the interfaces, *Langmuir*, 1999, *15*, 4630-4635.

[81] Y. Lu, H. Xiong, X. Jiang, Y. Xia, M. Prentiss, G. M. Whitesides, Asymmetric dimers can be formed by dewetting half-shells of gold deposited on the surfaces of spherical oxide colloids. *J. Am. Chem. Soc.* 2003, *125*, 12724-12725.

[82] Z. Bao, L. Chen, M. Weldon, E. Chandross, O. Cherniavskaya, Y. Dai, J. Tok, Toward controllable self-assembly of microstructures: Selective functionalization and fabrication of patterned spheres. *Chem. Mater.* 2002, *14*, 24-26.

[83] A. Perro, S. Reculusa, S. Ravaine, E. Bourgeat-Lami, E. Duguet, Design and synthesis of Janus micro- and nanoparticles. *J. Mater. Chem.* 2005, *15*, 3745-3760.

[84] L. Hong, A. Cacciuto, E. Luijten, S. Granick, Clusters of charged Janus spheres, *Nano Lett.* 2006, *6,* 2510-2514.

[85] G. Zhang, D. Wang, H. Möhwald, Patterning microsphere surfaces by templating colloidal crystals. *Nano Lett.* 2005, *5*, 143-146.

[86] G. Zhang, D. Wang, H. Möhwald, Nanoembossment of Au patterns on microspheres. *Chem. Mater.* 2006. *18,* 3985-3992.

[87] A. B. Pawar, I. Kretzschmar, Patchy particles by glancing angle deposition. *Langmuir* 2008, *24*, 355-358.

[88] G. Zhang, D. Wang, H. Möhwald, Decoration of microspheres with gold nanodots—giving colloidal spheres valences. *Angew. Chem. Int. Ed.* 2005, *44*, 7767-7770.

[89] D. R. Nelson, Toward a tetravalent chemistry of colloids. *Nano Lett.* 2002, *2*, 1125-1129.

[90] J. Pacifico, D. Gómez, P. Mulvaney, A simple route to tunable two-dimensional arrays of quantum dots. *Adv. Mater.* 2005, *17*, 415-418.

[91] J. Pacifico, J. Jasieniak, D. E. Gómez, P. Mulvaney, Tunable D-3 arrays of quantum dots: Synthesis and luminescence properties. *Small* 2006, *2*, 199-203.

[92] D. S. Sutherland, M. Broberg, H. Nygren, B. Kasemo, Influence of nanoscale surface topography and chemistry on the functional behaviour of an adsorbed model macromolecule. *Macromol. Biosci.* 2001, *1*, 270-273.

[93] C.-W. Kuo, J.-Y. Shiu, P. Chen, Size- and shape-controlled fabrication of large-area periodic nanopillar arrays. *Chem. Mater.* 2003, *15*, 2917-2920.

[94] C.-W. Kuo, J.-Y. Shiu, Y.-H. Cho, P. Chen, Fabrication of large-area periodic nanopillar arrays for nanoimprint lithography using polymer colloid masks. *Adv. Mater.* 2003, *15*, 1065-1068.

[95] S. M. Weekes, F. Y. Ogrin, W. A. Murray, Fabrication of large-area ferromagnetic arrays using etched nanosphere lithography. *Langmuir* 2004, *20*, 11208-11212.

[96] S. Han, Z. Hao, J. Wang, Y. Luo, Controllable two-dimensional photonic crystal patterns fabricated by nanosphere lithography. *J. Vac. Sci. Technol. B* 2005, *23*, 1585-1588.

[97] K. Ryu, A. Badmaev, L. Gomez, F. Ishikawa, B. Lei, C. Zhou, Synthesis of aligned single-walled nanotubes using catalysts defined by nanosphere lithography. *J. Am. Chem. Soc.* 2007, *129*, 10104-10105.

[98] K. H. Park, S. Lee, K. H. Koh, R. Lacerda, K. B. K. Teo, W. I. Milne, Advanced nanosphere lithography for the areal-density variation of periodic arrays of vertically aligned carbon nanofibers. *J. Appl. Phys.* 2005, *97*, 024311.

[99] X. Wang, C. J. Summers, Z. L. Wang, Large-scale hexagonal-patterned growth of aligned ZnOnanorods for nano-optoelectronics and nanosensor arrays. *Nano Lett.* 2004, *4*, 423-426.

[100] B. Fuhrmann, H. S. Leipner, H.-R. Höche, L. Schubert, P. Werner, U. Gösele, Ordered arrays of silicon nanowires produced by nanosphere lithography and molecular beam epitaxy. *Nano Lett.* 2005, *5*, 2524-2537.

[101] J. G. C. Veinot, H. Yan, S. M. Smith, J. Cui, Q. Huang, T. J. Marks, Fabrication and properties of organic light-emitting "nanodiode" arrays. *Nano Lett.* 2002, *2*, 333-335.

[102] J. M. Yao, A. P. Le, S. K. Gray, J. S. Moore, J. A. Rogers, R. G.L Nuzzo, Functional Nanostructured Plasmonic Materials. *Adv. Mater.*2010, *22*, 1102-1110.

[103] Large-area high-quality plasmonic oligomers fabricated y angle-controlled coilloidal nanolithography. *ACS Nano*2011, *5*, 9009-9016.

[104] J. Aizpurua, P. Hanarp, D. S. Sutherland, M. Kall, G. W. Bryant, F. J. Garcia de Abajo, Optical properties of gold nanorings. *Phys. Rev. Lett.* 2003, *90*, 057401.

[105] P. Hanarp, M. Kall, D. S. Sutherland, Optical properties of short range ordered arrays of nanometer gold disks prepared by colloidal lithography. *J. Phys. Chem. B* 2003, *107*, 5768-5772.

[106] B. Lamprecht, G. Schider, R. T. Lechner, H. Ditlbacher, J. R. Krenn, A. Leitner, F. R Aussenegg, Metal nanoparticle gratings: Influence of dipolar particle interaction on the plasmon resonance. *Phys. Rev. Lett.* 2000, *84*, 4721-4724.

[107] J. Liu, A. I. Maaroof, L. Wieczorek, M. B. Cortie, Fabrication of hollow metal "nanocaps" and their red-shifted optical absorption spectra. *Adv. Mater.* 2005, *17*, 1276-1281.

[108] Y. Lu, G. L. Liu, J. Kim, Y. X. Mejia, L. P. Lee, Nanophotonic crescent moon structures with sharp edge for ultrasensitive biomolecular detection by local electromagnetic field enhancement effect, *Nano Lett.* 2005, *5*, 119-124.

[109] Y. Yao, J. Yao, V. K. Narasimhan, Z. Ruan, C. Xie, S. Fan, Y. Cui, Broadband light management using low-Q whispering gallery modes in spherical nanoshells. Nat. Commun. 3:664.

[110] L. Li, Y. Li, S. Gao, N. Koshizaki, Ordered Co_3O_4 hierarchical nanorod arrays: tunable superhydrophilicity without UV irradiation and transition to superhydrophobicity. J. Mater. Chem. 2009, 19, 8366-8371.

[111] A. Moser, K. Takano, D. T. Margulis, M. Albrecht, Y. Sonobe, Y. Ikeda, S. Sun, E. E. Fullerton, Magnetic recording: advancing into the future. *J. Phys. D* 2002, *35*, R157-167.

[112] J. Zhu, Y. Zheng, G. A. Prinz, Ultrahigh density vertical magnetoresistive random access memory. *J. Appl. Phys.* 2000, *87*, 6668-6673.

[113] F. Zhu, D. Fan, X. Zhu, J.-G. Zhu, R. C. Cammarata, C.-L. Chien, Ultrahigh-density arrays of ferromagnetic nanorings on macroscopic areas. *Adv. Mater.* 2004, *16*, 2155-2159.

[114] M. Albrecht, G. Hu, I. L. Guhr, T. C. Ulbrich, J. Boneberg, P. Leiderer, G. Schatz, Magnetic multilayers on nanospheres. *Nature Mater.* 2005, *4*, 203-206.

[115] Q. Chen, E. Diesel, J. K. Whitmer, S. C. Bae, E. Luijten, S. Granick, Triblock colloids for directed self-assembly. *J. Am. Chem. Soc.* 2011, *133*, 7725-7727.

[116] Q. Chen, S. C. Bae, S. Granick, Directed self-assembly of a colloidal kagome lattice. *Nature* 2011, *469*, 381-384.

IntechOpen